ANTIGEN PRESENTING CELLS IN THE RETINA

A DISSERTATION
SUBMITTED TO THE FACULTY OF THE GRADUATE SCHOOL
OF THE UNIVERSITY OF MINNESOTA
BY

UTE LEHMANN

IN PARTIAL FULFILLMENT OF THE REQUIREMENTS
FOR THE DEGREE OF
DOCTOR OF PHILOSOPHY

DALE S. GREGERSON

SEPTEMBER 2010

COPYRIGHT

ACKNOWLEDGEMENTS

Thanks to everyone who helped me on my way to fulfill my life's dream of becoming a scientist.

DEDICATION

This dissertation is dedicated to my grandmother, Annemarie Lehmann, who always believed in me.

ABSTRACT

The presence and activity of dendritic cells (DC) in retina is controversial. This is in part due to the limited number of DC in the retina and the small number of reliable DC markers. In addition, functions ascribed to DC in other parts of the body are thought to be done by microglia in the central nervous system. CD11c is the cellular marker most associated with DC. In order to study the nature of retinal DC, transgenic mice that express green fluorescent protein (GFP) on the CD11c promoter were used to visualize, quantify, and characterize DC in both quiescent and injured retinas. In the quiescent retina it was found that compared to the number of neurons and microglial cells there were relatively few DC located in the nerve fiber layer and the outer plexiform layer. Upon retinal injury by either optic nerve crush or exposure to continuous bright light, the numbers of DC increased significantly and translocated to retinal layers associated with the injury. Surprisingly, the retinas of the eyes contralateral to the optic nerve crush also showed a significant increase in DC. The potential origin of the DC in retina was examined using a chimeric mouse paradigm. Most of the retinal DC were found to originate from circulating precursors, and a smaller number from a local progenitor cell population. This study suggests that retinal DC are a previously overlooked population, distinct from microglia, and may be important in the injury response and maintenance of homeostasis in the retina.

TABLE OF CONTENTS

LIST OF TABLES

LIST OF FIGURES

INTRODUCTION

The Presentation of Antigen

A central event in adaptive, antigen-specific immunity is the recognition by naïve T cells of cognate antigen on antigen presenting cells (APC). Antigen presentation is the process by which both foreign and self-antigens are processed and displayed in either class I or class II in the major histocompatibility complex (MHC) molecules on the cell surface in order to generate the appropriate effector or tolerogenic responses in T cells (1, 2). Normal physiological processes require that antigens be processed before they can be recognized by T cells. For many exogenous extracellular antigens, such as those associated with bacteria, this process involves the ingestion of the antigen by APC via endocytosis. Once inside the APC the endosome fuses with a lysosome where the antigen is degraded into short peptides of 7-12 amino acids. These antigenic peptides are then loaded onto class II histocompatibility molecules (MHC class II) in the endoplasmic reticulum (ER) and are then transported to the plasma membrane and displayed at the cell surface. It is there that they can be recognized by antigen specific $CD4^+$ T cells (Fig.1). Many endogenous intracellular antigens, including self-antigens, and viral antigens, are degraded in proteasomes and are then picked up by transporter associated with antigen processing (TAP) proteins in the ER. There the peptides are loaded onto MHC class I molecules. The peptide-loaded MHC class I molecule then leaves the ER through the secretory pathway to reach the cell surface, where they can be recognized by $CD8^+$ T cells (Fig. 2) (3-5).

APC have been described as being either professional or non-professional. Professional APC are derived from hematopoietic progenitors, which are characterized by expression of CD45, and are very efficient at internalizing antigen and then displaying peptides in MHC class II or I on their surface. Professional APC are also characterized by the expression of T cell receptor ligands and a wide range of co-stimulatory signals that are required for the activation of naïve T cells (6). In contrast, non-professional APC are not derived from hematopoietic progenitor cells and are unable to induce primary responses in naïve T cells. However, under certain circumstances they can display antigen and generate signals necessary for a T cell response (7). Non-professional APC also serve as targets of antigen specific effector T cells in secondary immune responses and include glial cells (brain), pancreatic beta cells, fibroblasts (skin), thymic epithelial cells, thyroid epithelial cells, and vascular endothelial cells.

A Professional's Professional: The Dendritic Cell

The three major types of professional APC are dendritic cells (DC), B cells, and macrophages. Of these, DC have the broadest range and most potent antigen presentation functions (8-10). In the 1970's, Steinman and Cohn coined the term "dendritic cell" to describe an adherent nucleated cell, characterized by many dendrites, that was found in the spleen of mice (11). Subsequently, it was demonstrated that DC were able to initiate T-cell immune responses (12). However, the study of DC was very limited as the DC population in the mouse spleen makes up only 1% of all nucleated cells (13) and there is a paucity of markers that distinguish them from monocytes/macrophages.

The 1990s were characterized by an explosion in the field of DC immunobiology as the enrichment of DC in large quantities was made possible from blood and bone marrow. It was then determined that specific cytokine mixtures containing granulocyte-monocyte colony-stimulating factor (GM/CSF), granulocyte colony-stimulating factor (G/CSF) (14, 15), and the FLT-3 ligand, a hematopoietic growth factor that induces dendritic cell expansion *in vivo*, led to the expansion of specific DC subsets in vitro (16, 17).

Recent work showed that there are a number of discrete DC cell lineages, derived from either myeloid (18) or lymphoid progenitors that reside in the bone marrow (Fig 3). DC, that have derived from lymphoid progenitors are called plasmacytoid DC (pDC) and are characterized by the expression of CD11c, B220, BST-2 (mPDCA), Toll Like Receptor (TLR) 7, and TLR 9 and the absence of CD11b (19). There is evidence that pDC are able to produce interferon-alpha and differentiate into myeloid DC upon virus infection (20). Plasmacytoid DC tend to favor a T helper cell 2 (Th2) response (21) and can drive T regulatory differentiation when they are either immature or mature (22). It was found that pDC make up only a small proportion of the total DC population.

Emigration of myeloid cells from the circulation into many tissues has been extensively studied (23), and shows that a major source of myeloid DC are monocytes (24). Myeloid DC can be distinguished from other cells by their expression of CD11c, CD11b, DEC205, 33D1, toll like receptor 2 (TLR 2), and TLR 4 on their surface. In vivo (25) and in vitro (26) studies have shown that precursors of myeloid DC can polarize T cell

effector responses toward Th1 or Th2. In addition, immature myeloid DC are able to function as regulatory DC (27). In contrast to pDC, myeloid DC make up the majority of the total DC population, and they have been detected in murine retina and the central nervous system (CNS) (28).

Antigen Presentation in the CNS

Several types of bone marrow (BM)-derived $CD45^+$ cells participate in immunity and inflammation in the CNS, including perivascular cells (PVC), microglia (MG), and dendritic cells (DC) (Fig. 4) (29-33). As discussed above DC are the most potent APC. Thus, confusion arose as the majority of $CD45^+$ cells in the CNS are MG, and there is little evidence supporting their antigen presenting ability.

MG are the major population of $CD45^+$ cells in the CNS, comprising 98% of the myeloid cells in the retina. MG are small, migratory, interstitial non-neural cells that form part of the adventitial structure of the CNS. They act as phagocytes and remove debris left by dead and dying neurons and glial cells (34, 35). With their wide array of functions, some consider MG to be comprised of several subpopulations, including cells with APC activity (36). Part of the uncertainty is rooted in the use of models in which the neural injury, or inflammation, is extensive, making it difficult to distinguish resident MG from infiltrating myeloid cells.

In addition to their ability to scavenge dead or dying neurons (37), MG have been reported to promote survival of damaged neurons (38) and to kill injured or excess neurons during development (39, 40), suggesting that the innate immune system can be protective or pathogenic in neural injuries and neurodegeneration (41). However, promoting recruitment of hematopoietic progenitor cells (HPC) into retina by systemic administration of G/CSF and erythropoietin (EPO) yielded retinal cells that assumed a MG morphology and phenotype. These cells were responsive to CXCL12, and reduced the rate of retinal degeneration in *rd1* mice (42), exhibiting neuroprotective function. However, their identity as resident MG is debatable. It is also reported that myeloid progenitor cells promoted retinal vascularization in a murine model of hyperoxia-induced ischemic retinopathy (43).

Recently, it was shown that purified $CD45^{+}$ cells from retina had little ability to present antigen to naïve T cells in vitro (30). In contrast, $CD45^{+}$ cells from brain, isolated by a similar procedure, were potent APC, providing antigen-dependent activation of naïve T cells (30). To explain the observed differences in antigen presentation, the $CD45^{+}$ cells from retina and brain were analyzed for differences in their phenotype. It was found that $CD11c^{hi}$ cells were virtually absent from retina, but prominent in the $CD45^{hi}$ subset of the brain (30). This result may be explained by the pervasive contamination of CNS tissue with meninges-derived $CD11c^{+}$ DC (44).

Autoimmune Models as Evidence for APC in the CNS

Several well-known animal models are used to study immune responses in nervous system tissue. Most of them are based on autoreactive, pathogenic CD4 and CD8 T cells specific for neural antigens and include experimental autoimmune uveoretinitis (EAU) (45-48), and experimental autoimmune encephalomyelitis (EAE) (49). The cells, which present antigen in the initial stages of immune recognition in the CNS, especially the retina, are not well characterized, but candidates have been identified (32, 33, 50-52).

Nevertheless, the ability to induce EAU in the retina implies that there is local recognition of antigen and on-going T cell activation. In earlier studies in the laboratory, recruited APC were able to support the induction of EAU (53). This outcome suggested that the small number of cells with a DC-like phenotype and function in quiescent retina limited the potency of the autoimmune response; it may also be true that their function as APC was altered by the immune privileged environment of the retina.

Immune privileged sites are tissues that are capable of local suppression or modulation of immune responses in order to protect vital structures. Immune privileged sites include: brain, parts of the eye (retina, cornea, and anterior chamber), testicles, placenta, and fetus (54, 55). The lack of lymphatic drainage in some of these tissues reduces the immune system's ability to process and present tissue-specific antigens from these sites.

Other known factors that contribute to the maintenance of immune privilege include: the blood/brain or blood/retinal barrier; the low expression of classical MHC class Ia molecules; the expression of immunoregulatory nonclassical, low polymorphic class Ib MHC molecules; the increased expression of surface molecules that inhibit complement activation; the local production of immunosuppressive cytokines, such as transforming growth factor beta (TGF-β); the presence of immunoregulatory neuropeptides; and the constitutive expression of membrane bound Fas ligand that controls the entry of Fas-expressing lymphoid cells (56, 57).

Controversy over DC Presence in the Retina

There is significant controversy as to whether DC exist in quiescent retina and function as APC. DC in quiescent retina have been difficult to study for phenotype, function, and origin, given the very low density of cells with DC markers. Conversely, evidence for DC in the inflamed retina has been readily found in the inflammatory infiltrates associated with the EAU model for retinal autoimmune disease (58). However, their relationship to DC in quiescent retina is unclear. The relationship between MG and DC is uncertain, and it is not clear whether retinal DC or other cells with APC ability are derived from MG, recruited from the circulation (53), or derived from local hematopoietic progenitor cells. Part of the difficulty is that normal retina has a low density of DC, and there are few markers for elucidation of their phenotype, function and origin. Of several markers associated with murine DC, CD11c is most frequently used. However, antibodies to murine CD11c are difficult to use in immunohistochemistry. Using flow cytometry and

antibodies 33D1 (59) and CD205, a small number of MHC class II^+ putative DC were identified in retina (32, 60).

Statement of Hypothesis

It is proposed here that the retina contains myeloid DC that are distinct from retinal MG, and these myeloid DC are the first responders to retinal injury. The following study describes a number of experiments that attempt to identify and characterize APC in the retina according to their origin, location, and their function.

Justification of Model

The models used in the proposed studies are advantageous for the determination of the origin, location, and function of retinal APC. First, using retina for our studies allows us to study pure CNS parenchyma without contamination by meninges. The meninges are a system of connective tissue membranes that envelop the CNS; the meninges are rich in immune cells leading to uncertain contamination of CNS parenchyma (44). Second, to visualize and study the responses of retinal DC, I took advantage of a transgenic mouse line (CD11c-DTR) where $CD11c^+$ DC express both the diphtheria toxin receptor (DTR) and green fluorescent protein (GFP) under the CD11c promoter (Fig. 5) (61). This mouse model allows the identification of DC by their expression of GFP and provides a method for the selective depletion of DC by treating the mice with diphtheria toxin (DTx). Third, the response of retinal DC to neural injury was examined by analysis of changes in the number and localization of DC following two distinct retinal injuries that do not disrupt

the blood retina barrier. The first retinal injury model looked at DC changes in both eyes that occurred after a unilateral optic nerve crush. This model was chosen as it perturbs the system without damaging the retinal architecture. The axonal damage induced by an optic nerve crush leads to retinal ganglion cell (RGC) death, and triggers a retinal MG response (62-66). The second retinal injury model studied the effects of light-induced retinal damage on DC. Constant light is a well-known model of injury to the retinal photoreceptor cells (67). Both injury models resulted in increased numbers of retinal GFP^+ DC in areas of the retina associated with the injured cells. Thus, both quiescent DC and activated DC in the retina could be characterized and their origin studied.

Figure 1. The MHC class II pathway.

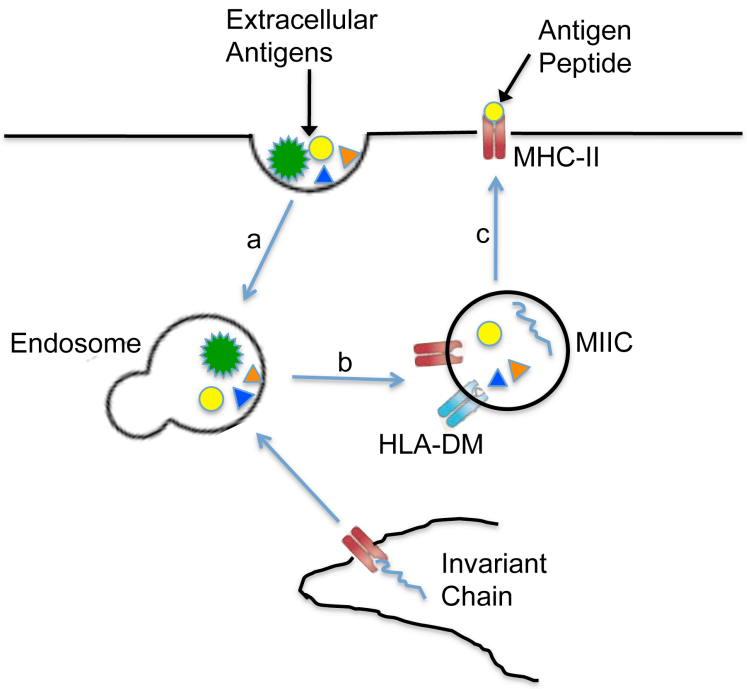

Figure 1. The MHC class II pathway. Exogenous extracellular antigens are taken up by macropinocytosis and enter the endosomal pathway. Once inside, the endosome fuses with a lysosome where the antigen is degraded into short peptides of 7-12 amino acids (a). These antigenic peptides are then loaded onto class II histocompatibility molecules (MHC class II) in the endoplasmic reticulum (b) with the help of HLA-DM, and are then transported to the plasma membrane and displayed at the cell surface (c). It is there that they can be recognized by antigen specific $CD4^+$ T cells. HLA-DM, intracellular protein that is involved in peptide presentation by MHC class II; MIIC, MHC class II compartment, specialized for loading peptides onto class II molecules.

Figure 2. The MHC class I pathway.

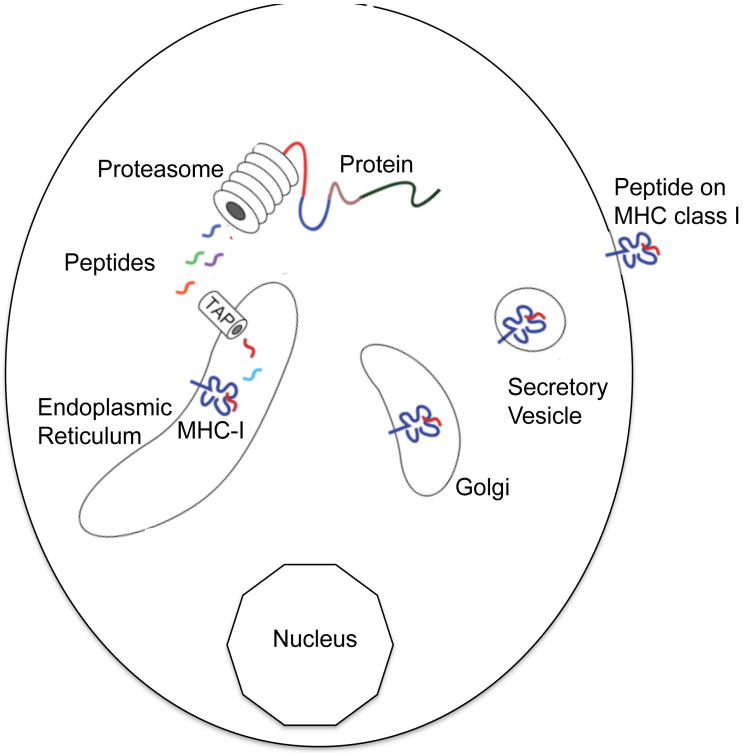

Figure 2. The MHC class I pathway. Endogenous intracellular antigens, including self-antigens and viral antigens, are degraded in proteasomes and are then picked up by transporter associated with antigen processing (TAP) proteins in the ER. There the peptides are loaded onto MHC class I molecules. The peptide-loaded MHC class I molecule then leaves the endoplasmic reticulum through the secretory pathway to reach the cell surface, where they can be recognized by $CD8^+$ T cells.

Figure 3. The Hematopoietic System.

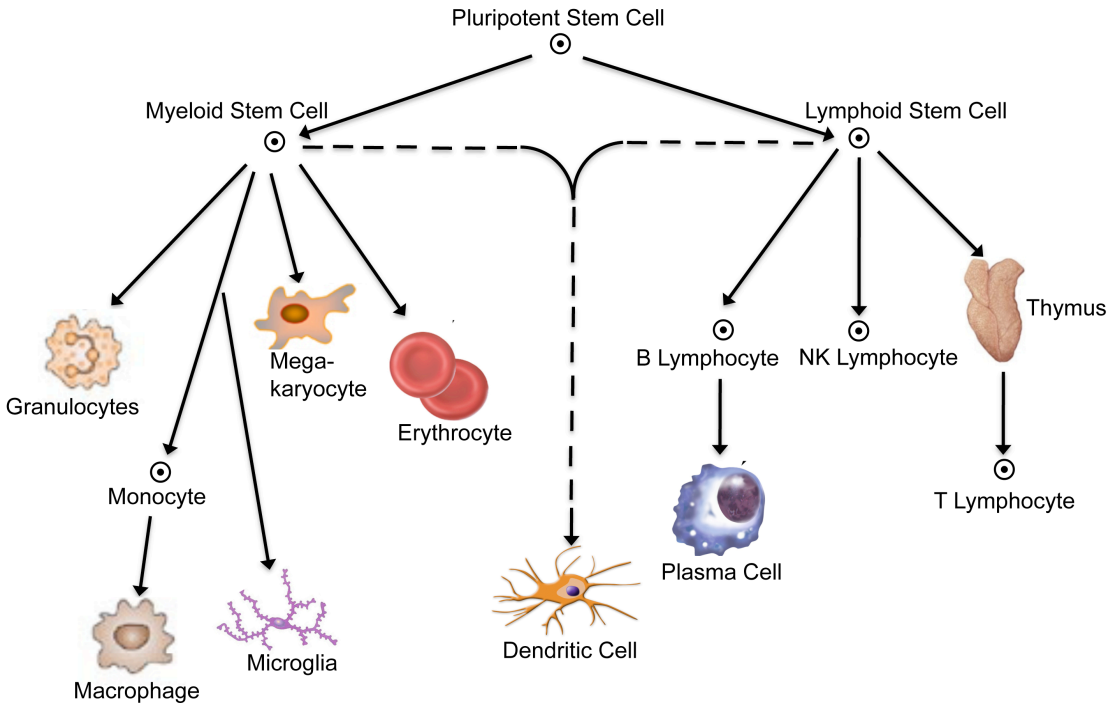

Figure 3. The Hematopoietic System. Dendritic cells can develop from either myeloid or lymphoid progenitor cells.

Figure 4. Schematic diagram of a retina demonstrating the major populations of cells and their approximate location.

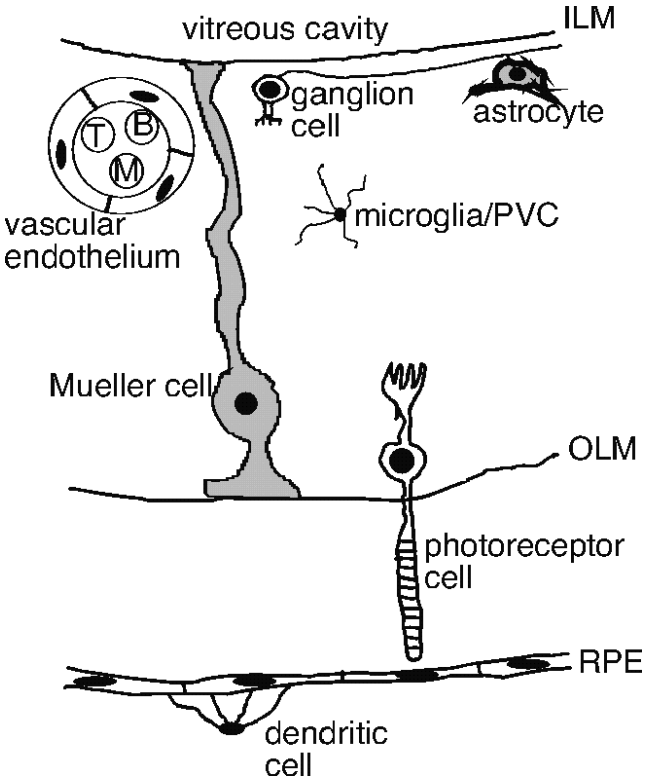

Figure 4. Schematic diagram of a retina demonstrating the major populations of cells and their approximate location. ILM, inner limiting membrane; PVC, perivascular cell; OLM, outer limiting membrane; RPE, retinal pigment epithelium

Figure 5. CD11c-DTR mice construct.

Figure 5. CD11c-DTR mice construct. The construct consists of a CD11c promoter, which is linked to a chimeric protein containing green fluorescent protein (GFP) and the primate diphtheria toxin receptor (DTR). Diphtheria toxin (DTx) selectively depletes $GFP^{+}(CD11c^{+})$ cells in these mice.

MATERIALS AND METHODS

Mice

All mice were on the B6 background. CD11c-DTR transgenic mice express a chimeric protein comprised of GFP and the DTR using the CD11c promoter (61). B6 CD45.1 and CD11c-DTR CD45.2 mice were used to allow the presence and extent of chimerism to be determined by flow cytometry. Mice were handled in accordance with the ARVO Statement for the Use of Animals in Ophthalmic and Vision Research, and University of Minnesota IACUC guidelines.

Immunostaining of Retinal Wholemounts

Mice were euthanized by CO_2 inhalation, and perfused with 12 mL of 2 U/mL heparin in Dulbecco's Phosphate-Buffered Saline (DPBS) to remove circulating $CD45^+$ cells in the vasculature. The retinas were removed as described by Winkler (68), and fixed in 4% paraformaldehyde for 12 min. Tissues were washed 3 times with DPBS for 5 min each. After washing, the retinas were blocked in 10% normal donkey serum (Jackson Immuno Research) with 0.1% Triton X-100 for 1 h at RT. Tissues were incubated overnight at 4 ^oC with primary antibody (CD45, BD Pharmingen; CD11b, clone M1/70, BD Pharmingen; rabbit anti-GFP, Invitrogen; β3-tubulin, clone TU-20, Abcam; MHC-II, clone M5/114, eBioscience). Retinas were washed again 3 times with DPBS for 5 min each. Secondary antibody (biotinylated anti-rabbit IgG, Vector; biotinylated anti-rat IgG, Vector; AF 488/Streptavidin, Invitrogen; AF 594 anti-rat IgG, Invitrogen; AF 405/Streptavidin, Invitrogen; AF 488 anti-mouse IgG, Invitrogen) was added and the

tissues were incubated for 3 h at room temperature. In some experiments, fluorescent-conjugated isolectin B_4 (Invitrogen) was included with the secondary antibodies to stain for vascular endothelial cells. Once more, the tissues were washed 3 times with DPBS and flat mounted, vitreous side up, onto slides. All immunostained retinal flatmounts were examined using a confocal scanning laser microscope (Olympus FluoView 1000, IX81 Inverted Confocal, Japan). Z-stacks of confocal images were reconstructed and analyzed using ImageJ software (National Institutes of Health, USA).

Optic Nerve Crush Injury

An ONC was done following anesthesia with ketamine/xylazine (87 mg/Kg : 13 mg/Kg) given IM. 0.5% proparacaine drops were applied topically. A lateral canthotomy was made to access the posterior pole. The conjunctiva was incised laterally and peeled back to the posterior segment. The optic nerve was exposed by gentle blunt-dissection of surrounding muscle bundles with watchmaker forceps. The nerve was partially clamped for 4 sec, 2 mm from the posterior pole of the globe with self-closing forceps (66) to obtain a consistent injury. Sham-operated controls were done similarly, except that the forceps were not allowed to close on the nerve.

Light Injury

The mice were exposed to constant light (3.6×10^3 lux) for four days. Some shade was available under their food and water supply, or when the mice were huddled together. The pupils were not dilated and the lids were not retracted. Light intensity was measured

using a Sekonic Auto-Lumi L-158 light meter. After light exposure, the mice recovered in normal cyclic light for 3 days. The retinas were harvested, and stained for GFP^+ cells and blood vessels.

Flow Cytometry

Mice were euthanized, perfused, and retinas removed as described above. The retinas were dissociated using Liberase/Blendzyme3 (Roche) and DNAse. The dissociated retinas were washed with DPBS and incubated for 10 min at room temperature in 100 µL FACS buffer (DPBS with 2% FBS and 0.02% sodium azide) containing 0.5 µg anti-mouse CD16/CD32 (Fc block). 0.5 to 4 µL of the appropriate fluorescent-labeled antibodies (eBioscience and BD) were added and incubated for 20 min on ice. Cells were washed, resuspended in FACS buffer and collected using a FACSCalibur and CellQuest software (BD Biosciences) and analyzed using CellQuest or FlowJo (TreeStar, Ashland, OR) software.

Intraocular DTx Treatment

Anterior chamber inoculation was done by a transcorneal deposition into the anterior chamber (AC) of the eye. Mice were anesthetized with ketamine (87 mg/kg) and xylazine (13 mg/kg) given intramuscular, followed by 0.5% proparacaine eye drops. The pupil was dilated with 1 % tropicamide eye drops. The tip of a 30 gauge needle was used at a shallow angle to put a slit into the cornea near the limbal-scleral junction. Approximately 1 µL of aqueous humor was allowed to escape. A 33 gauge blunt canula attached to a 10

μL Hamilton syringe was used to slowly pass 1 – 1.5 μL of saline or DTx (5 ng) into the AC.

Preparation of DC and Monocytes

Fresh $CD11c^+$ DC were prepared from a suspension of pooled bone marrow (BM) cells by positive selection with CD11c paramagnetic beads and an LS column (Miltenyi Biotec, Inc., Auburn, CA, per manufacturer's recommendations). $CD11b^+$ monocytes were prepared from a suspension of pooled BM cells that were first depleted with Abs to CD19 and CD11c using magnetic cell separation over LD columns (Miltenyi Biotec, Inc.). The flow-through cells were then positively selected for monocytes using $CD11b^+$ beads over LS columns.

APC Activity Assay in B6 Mice

Mice were euthanized by CO_2 inhalation, and perfused with 12 mL of 2 U/mL heparin in DPBS to remove circulating $CD45^+$ cells in the vasculature. The retinas were removed as described by Winkler (68) and dissociated using Liberase/Blendzyme3 and DNAse as described above. For $CD45^+$ enrichment, the washed, dissociated retinal cells were incubated with paramagnetic anti-CD45 and positively selected on a MACS LS columns (Miltenyi). Selected cells were flow sorted for GFP^+CD11b^+ and GFP^-CD11b^+ cells using BD FACS Aria. The appropriate number of sorted APC was pipeted into 96 well plates. Antigen (0.5 mM, Biomedical Genomics Center University of Minnesota, SVTLPAASHAIPHLT-amide) and naïve BG2 CD4 T cells ($2x10^4$/well), expressing the

βgal-specific TCR and GFP under the Foxp3 promoter, and IL-2 (2.5 ng/mL) were added. The plates were incubated at 37^{o}C for 4 days. Cells were collected and incubated for 10 min at room temperature in 100 μL FACS buffer (PBS with 2% FBS and 0.02% sodium azide) containing 0.5μg anti-mouse CD16/CD32 (Fc block). 0.5 to 3 μL of the appropriate fluorescent-labeled antibodies (eBioscience and BD Biosciences) were added and incubated for 20 min on ice. Cells were washed, resuspended in FACS buffer and collected using a FACSCalibur and CellQuest software (BD Biosciences) and analyzed using CellQuest or FlowJo (TreeStar, Ashland, OR) software.

Cell Chamber Assay

Mice were euthanized, perfused, and retinas removed as described above. For CD45^{+} enrichment, the washed, dissociated retinal cells were incubated with paramagnetic anti-CD45 and positively selected on MACS LS columns (Miltenyi). Approximately 5000 retinal CD45^{+} cells were added to each cell chamber containing 200mL of X-VIVO 15 medium (LONZA). Each chamber was treated with different cytokines or combinations of them, i.e. GM/CSF 5ng/mL, INF-γ 10 ng/mL. Bone marrow cells were used as control. Tibias and femurs were harvested and the bone marrow was flushed out with 1X DPBS. To break up clumps the marrow was passed through a 70μm mesh filter and resuspended in CMF-PBS. Approximately 5x10^{3} bone marrow cells were added to each cell chamber containing 200mL of medium. Cell chambers containing BM cells received the same treatment that was applied to retinal cells. Between day 1 and day 5 post-seeding the cells were stained for GFP and CD11b expression. The cells were fixed in 4%

paraformaldehyde for 10 min. Cells were washed briefly with DPBS. After washing, the cells were blocked in normal donkey serum (Jackson Immuno Research Laboratories, Inc., West Grove, PA) with 0.5% Triton X-100 for 15 min at RT. Cells were incubated overnight at 4^{o}C with primary antibody (CD11b, M1/70, BD Pharmingen; rabbit anti-GFP, Invitrogen). Cells were washed 3 times briefly with DPBS. Secondary antibody (anti-rat AF 594, Invitrogen; anti-rabbit AF 488, Invitrogen) was added and the cells were incubated for 3 h at room temperature. Once more, the cells were washed 3 times briefly with DPBS and cover slipped. Mounting medium (Vector) contained DAPI. All immunostained cells were examined by fluorescent microscopy (LEICA DMR).

Preparation of Radiation Bone Marrow Chimeras (RBMC)

Mice were sacrificed by CO_2 inhalation. Tibias and femurs were harvested and the bone marrow was flushed out with 1X DPBS. The marrow suspension was passed through a 70μm mesh filter and resuspended in CMF-PBS. Red blood cells were lysed in NH_4Cl. Recipient mice were irradiated as specified before the bone marrow cells were administered *iv*. Lead shielding (2.5 cm, which attenuates the Cs^{137} beam by 90%) was used where indicated to selectively protect either the head or the trunk/limbs from irradiation.

Statistics

ANOVA, performed by InStat software, were used to statistically evaluate differences in T cell activation and T regulatory cell generation between retinal GFP^{+} and GFP^{-} cell

populations in treated and untreated CD11c-DTR mice. Student's t-tests were used for other comparisons.

RESULTS

Morphology and Distribution of GFP^+ DC in Retina.

Since a small number of putative DC has been reported in quiescent retina by immunofluorescence (50) and by flow cytometry (60), retinas from the CD11c-DTR mouse, where the DC express GFP from a CD11c promoter, were examined for the presence of GFP-positive cells. These GFP-positive cells are putative DC as evidenced by expression of the GFP reporter due to activity of the CD11c reporter, and subsequently will be referred to as GFP^+ DC. As found for many GFP-expressing mice, the GFP expression level does not give robust autofluorescence for microscopy. Thus, immunostaining with a polyclonal rabbit antibody to GFP was used to detect the GFP positive cells in retinal wholemounts with high sensitivity. To facilitate examination and quantification of the laminar distribution, morphology and number of the GFP^+ DC, retinal wholemounts (Fig. 6) were double stained with anti-GFP and isolectin B_4, which labels blood vessels, and observed by confocal microscopy (Fig. 7). The GFP^+ DC had two distinct morphologies. Perivascular GFP^+ DC were found in the ganglion cell/nerve fiber layer (GCL/NFL) (Fig. 8), where they frequently exhibited a close association with large blood vessels (Fig. 7A). Highly ramified GFP^+ DC, without evidence of vascular association, were found among the extensively branched smaller blood vessels of the GCL (Fig. 7B). While some of the GFP^+ DC were associated with branch points in intermediate-sized vessels, these were relatively rare (Fig. 7C). Relative to the GCL and NFL, GPF^+ DC were rarely found in the inner plexiform layer (IPL) (Fig. 7D). None were found in the inner nuclear layer (INL). In aggregate, the inner layers of the mouse

retina, defined as the NFL, GCL, IPL, and INL, contained 38 ± 17 GFP^+ DC/retina. A similar number (57 ± 25) of ramified DC was found in the outer plexiform layer (OPL) (Fig. 7E), yielding a total of 95 ± 42 GFP^+ DC/quiescent retina (N = 14).

The position of GFP^+ DC was also compared in central and peripheral regions of the retina. When viewed in the cross-sectional plane, it was revealed that the ramified GFP^+ DC were remarkably two-dimensional (Fig. 9). The lateral distribution was highly variable; GFP^+ cells were found in the peripapillary region (Fig. 7F), peripheral retina (Fig. 7B), and the far periphery (Fig. 7G). Some were found as single cells in isolation, while others were found in small clusters in the periphery (Fig. 7H). This distribution differs from that of microglia (MG), which are well-known to be concentrated in the GCL/IPL, with a much smaller number in the OPL (69-71). In the CD11c-DTR mice, immunostaining for CD11b, a widely used marker for MG (Fig. 10), confirmed that the distribution of the CD11c-DTR/GFP^+ DC differed from that of the MG in these transgenic mice. The lateral distribution of the $CD11b^+$ cells was fairly uniform. The total number of GFP^+ DC was a small fraction (approximately 2 %) of the number of MG per retina (95 ± 42 GFP^+ DC; N = 14 compared to 4291 ± 545 $CD11b^+$ cells; N = 8) found in normal, quiescent retinas.

Characterization of Retinal GFP^+ DC.

To further characterize the retinal GFP^+ DC, expression of immunologically relevant molecules was examined in this population. Dual staining of retinal wholemounts for

CD11b and GFP revealed that all GFP^+ DC were also $CD11b^+$ (Fig. 11A-C, circled cells), raising the possibility that the subset of DC had been previously misidentified as $CD45^+CD11b^+$ MG. In addition, immunofluorescent staining of retinal wholemounts in the transgenic mice showed a small number of GFP^+ DC that were also MHC class II^+ and possessed a ramified morphology (Fig. 11D-F). The GFP^+ DC in quiescent retina had a much higher frequency of class II expression (4.4%) than did the GFP^- MG (0.2%) (Table 1). This finding is consistent as only mature DC, e. g. after in insult to the retina, express MHC class II. The results in Fig. 11D-F are not representative of the proportions of cells that stain for MHC class II and GFP, but demonstrated the reliability of the IF protocol, and its capacity for detecting double positive cells.

Further characterization of GFP^+ DC in the CD11c-DTR retina was performed by FACS analysis. The difficulty of immunostaining even lightly-fixed retinal sections or wholemounts with available antibodies for CD11c or CD45 were resolved in flow cytometry. Unlike lymphoid tissue, retinal tissue contained two distinct $CD45^+$ populations, one with high expression of CD45 ($CD45^{hi}$) and one with medium expression ($CD45^{med}$) (Fig 12A). The GFP^+ DC were concentrated in the $CD45^{med}$ population; the $CD45^{hi}$ population was GFP^- (Fig. 12B1 vs 12B2). Analysis of the $CD11c^+$ cells in the $CD45^{med}$ population showed that all $CD11c^+$ cells in normal CD11c-DTR retina were also $CD11b^+$ (Fig. 12C2), confirming our previous immunofluorescence results (Fig. 11). When $CD11c^+CD11b^+$ cells were analyzed for GFP expression, the GFP^+ cells were found to be a subpopulation of the $CD11c^+CD11b^+$ cells compared to *wt*

B6 mice controls (Fig. 12D2 vs 5D3). Although GFP expression was dependent on CD11c expression, the level of GFP expression in the retinal DC did not correlate with the level of CD11c expression (Fig. 12D; 1-3). This result prompted analysis to confirm the fidelity of the GFP expression on other populations of $CD11c^+$ cells. CD11c-DTR mouse lymphoid tissue was examined by flow cytometry and showed that GFP was expressed in the DC populations, and the expression levels of CD11c and GFP were well-correlated (Fig. 13).

Local Depletion of Retinal DC in CD11c-DTR Mice. Penetration of the Cornea Induces a Response in GFP^+ DC in the Retina.

CD11c-dependent expression of the DTR/GFP chimeric protein allows depletion of DC by injections of DTx. To confirm that the GFP^+ DC seen by flow cytometry were diphtheria toxin (DTx) sensitive and represented the GFP^+ DC seen by immuno-fluorescence, retinas from CD11c-DTR mice were examined 36 hr after intraocular injection of 5 ng DTx. FACS analysis showed that DTx was able to deplete these GFP^+ DC.

Our initial attempts to deplete retinal DC locally involved the injection of DTx, or saline only as a control, into the anterior chamber of murine eyes (Fig.14). Three important properties of retinal DC were revealed by this approach. First, the one-time injection of 1 ml saline alone led to a rapid decline in the number of GFP^+ DC in the retina of the injected eye on day 1 post-injection, followed by an increase in the number of GFP^+ cells

by day 4, and a return to normal numbers by day 10 (Fig. 15A). Since the retina was untouched by the needle in this type of injection, the mechanism of DC response is unclear. Second, the one-time injection of 1 ng DTx in 1 ml gives a GFP^+ DC response that is indistinguishable from the saline injection control (Fig. 15B). One might conclude that the DTx treatment was ineffective for depletion of the DC; however, after 4 consecutive injections of DTx or saline on days 0, 3, 6, and 9, complete depletion of GFP^+ DC was achieved while there was no change after the multiple saline injections. Third, repeated 1 ng DTx injections induced a substantial and sustained depletion of the GFP^+ DC, while repeated saline injections did not (Fig. 15C). The depletion of the GFP^+ DC following 2 consecutive injections of 5 ng DTx was confirmed by flow cytometry (Fig. 15D). The results of the anterior chamber injections, whether saline or DTx, suggested that retinal DC perform a highly sensitive surveillance function, in which they respond even to subtle changes in the retina. Apart from DC depletion, the mice appeared to be unaffected by the DTx injections, with no adverse effects on the retina or the mice even after the anterior chamber injections of up to 25 ng. The $CD11b^+$ MG were not depleted by repeated DTx treatment. Flow cytometry confirmed that the GFP^+ DC, which were approximately 2 % of the total $CD45^+$ cells, were lost after DTx treatment (Fig. 15D).

Injury Response of the Retinal DC.

To determine if the retinal GFP^+ DC population responded to a more direct injury to the retina, an optic nerve crush was performed on CD11c-DTR mice. An optic nerve crush

(ONC) damages axons of retinal ganglion cells and induces apoptosis in the injured RGC. The number of $TUNEL^+$ apoptotic RGC die over the next 2 weeks. FACS analysis showed that following optic nerve crush, GFP levels increased in the $CD11c^+CD11b^+$ subset of cells from the $CD45^{med}$ population (Fig. 12B1, D1). Immunofluorescence analysis confirmed a rapid and significant increase in GFP^+ DC numbers (Fig. 11A), with a 10-fold increase at day 9 in ipsilateral retinas of optic nerve crush-injured mice. Significantly increased numbers of GFP^+ DC ($p < 0.001$) were seen as early as day 2 post-optic nerve crush in the ipsilateral retina, and elevated numbers persisted at least 60 days. Interestingly, the number of GFP^+ DC in the contralateral retina increased with a lag of 1 – 2 days compared with the optic nerve crush-injured retina (Fig. 16A). Although not reaching the numbers found in the injured retina, the increase in the contralateral retina was still significantly greater than the number in normal control retina ($p < 0.001$, day 3). Sham-operated controls were normal in number, distribution, and morphology of $CD11c^+$ cells on days 9 and 20 post-crush injury (Fig. 16A).

Changes in morphology of GFP^+ DC were also found post-optic nerve crush. In the normal GCL, ramified and perivascular GFP^+ DC were seen (Fig. 16B, yellow arrows). A large increase in GFP^+ DC with an elongated morphology and a distinct radial orientation was found at 7 d post-optic nerve crush (not shown), and at 24 d post-optic nerve crush (Fig. 16C). Examination of unmanipulated contralateral eyes also revealed the presence of elongated GFP^+ DC, but to a lesser degree (Fig. 16D). The source of the radial pattern of GFP^+ staining was analyzed and was found to result from the association of GFP^+ DC

with the β3-tubulin$^+$ axons of the RGC (Fig. 17), which have a radial pattern converging at the optic nerve head. Examination of optical sections from different layers of a retina collected 10 d post-optic nerve crush revealed that the DC were closely associated with the nerve fibers of the RGC in the injured retina (Fig. 17A-C). This relationship is illustrated by examination of an enlargement of panel C, where DC can be seen wrapped around a nerve fiber (Fig. 17D-F). There was also an increase in GFP$^+$ DC numbers in the OPL (Fig. 17G-I), but there were no changes in DC morphology. This may be related to the absence of directly injured optic axons in this region.

Since MG greatly outnumber the DC in retina, it was important to ask if they were also found closely associated with the RGC axons. Staining retinal wholemounts post-crush injury for CD11b, GFP, and β3-tubulin showed that the majority of cells closely associated with nerve fibers were GFP$^+$CD11b$^+$ DC (Fig. 18A). Few CD11b$^+$GFP$^-$ MG were found; only 4 were present in the field shown (Fig. 18B, red arrows). Overall, 92.6% of the cells in close contact with the optic nerve fibers were GFP$^+$ DC.

To further confirm that the GFP$^+$ retinal DC differed from the MG, their sensitivity to DTx was examined. A single intraocular injection of 5 ng of DTx given 7 d post-optic nerve crush rapidly killed the GFP$^+$ DC responding in the RGC/NFL layers in the retina (Fig. 19C, D), but the underlying retina was normally populated with MG. The susceptibility of MG to multiple DTx treatments was evaluated in CD11c-DTR mice. Three injections at 2 day intervals gave a sustained reduction in the number of the GFP$^+$ DC in the uncrushed retina, from 95 ± 42 to 10 ± 15, while the number of GFP$^-$

$CD11b^+$MG was maintained. DTx treatment post-optic nerve crush also depleted the GFP^+ DC, from 95 ± 42 to 14 ± 14, but did not affect the number of GFP^-CD11b^+ MG, from 4291 ± 545 to 3971 ± 627 (Table 2). These mice were given an optic nerve crush to one eye and 13 d later were depleted of their GFP^+ DC by injecting 5 ng DTx into the anterior chamber of the injured eye. At 2 day intervals, the mice received two more injections of DTx. The retinas were harvested 2 d later and the numbers of GFP^+ DC and GFP^-MG determined. These results further demonstrated that the two populations were distinct.

Light Injury and the Retinal GFP^+ DC.

To determine if the DC response to retinal optic nerve crush injury was broadly representative of DC activity in the retina after injury, light-induced retinal damage was performed. Light-induced retinal injury is a well-known model used to study neural remodeling and mechanisms of resistance to light damage. It consists of maintaining the mice in constant light for at least 24 hours (67, 72-74). Unlike the ONC, which injures the axons of the RGC, light damage injures the photoreceptor cells. To determine if the GFP^+ DC responded to low level photoreceptor cell injury, CD11c-DTR mice were exposed to 3.6 x 10^3 lux (overhead) continuously for 4 days. This was followed by 3 days of normal 12 hour light/12 hour dark housing conditions. This continuous light exposure paradigm did not lead to detectable morphological damage to the retina when sampled 3 or 14 days post-light exposure (data not shown), consistent with the well-known resistant B6 phenotype (67). However, the GFP^+ DC substantially increased in number after this

continuous light exposure (Table 3). They were concentrated in the OPL and exhibited a ramified morphology (Fig. 20). The upregulation in DC numbers as an injury response appeared to reflect the location of the injured neurons.

MHC Class II Expression of DC Following Optic Nerve Crush.

Since significant changes in morphology and numbers of GFP^+ DC were seen after an optic nerve crush, MHC class II expression was examined as a marker of DC activation. At ten days post-optic nerve crush, retinal wholemounts were immunostained for GFP and MHC class II. Comparison of retinas from untreated and optic nerve crush-treated mice showed that MHC class II expression was dramatically upregulated on GFP^+ DC, but not on the MG (Fig. 21; Table 1). The frequency of MHC class II^+ DC in normal retina was quite low; 8 of 180 GFP^+ DC in quiescent retina were class II^+ (4.4%). Overall, approximately 15 cells/retina were MHC class II^+. In the same retinas, only 9 MG (GFP^-CD11b^+) were found to stain for MHC class II, approximately 0.2% of the total MG. After an optic nerve crush, 63 of 127 GFP^+ DC (49.6%) were class II^+, and MHC class II^+ MG were extremely rare (only 1 field contained a single positive cell in two retinas). Overall, an optic nerve crush injury led to the selective upregulation of MHC class II expression in the GFP^+ DC population.

Characterization of Retinal DC: APC Activity in DC and MG to CD4 T Cells.

Preliminary results showed that depletion of the DTR^+ DC by DTx treatment resulted in more severe EAU. This suggests that the role of the retinal DC may be

immunoregulatory, leading to inhibition of retinal inflammation and pathogenesis. To test this hypothesis, the ability of retinal DC to present antigen was assessed by flow cytometry analysis. Retinal GFP^+ DC from CD11c-DTR mice were co-cultured for 4 days with naïve BG2 CD4 T cells, expressing the β-gal T cell receptor (TCR) and backcrossed to the Foxp3-GFP mice which express GFP under the Foxp3 promoter. These T cells, together with β-gal peptide, and IL-2 were stimulated with purified retinal APC populations. Retinal APC were isolated either from mice that were untreated or mice that had received a unilateral optic nerve crush 7 days prior to harvest. Only the cells that expressed the highest level of GFP were used for culture, as these cells most likely to be the $CD11c^+$ cells. For GFP^- cells, the cells with the lowest fluorescence in the GFP/FITC channel were used for culture. All samples were stained with anti-CD44, anti-25, and anti-CD4. Cells were size-selected for increased forward scatter to focus on large, activated cells. Activated T cells were identified by the expression of CD44 and CD25, and the lack of expression of $Foxp3^-$. GFP was used to detect $Foxp3^+$ T regulatory cells within the examined cells. Analysis showed that the GFP^+ DC isolated from retinas treated with an optic nerve crush were the more potent population of retinal cells to activate T cells as compared to the GFP^- population from the same retina $P<0.001$ (Fig. 22). The GFP^- population of cells isolated from the crushed retinas did not activate T cells well. These cells were more potent in the generation of T regulatory cells as compared with the GFP^+ cells of the same retina, $P<0.001$ (Fig. 22).

Origin of Retinal DC: MG are Unable to Differentiate into DC-like Cells.

One potential source of DC in the retina is the MG. This hypothesis was tested in different ways. If the hypothesis is true, differentiated DC should form from the MG cells. MG, isolated by a combinationof Miltenyi magnetic bead separation and FACS, from two groups of CD11c-DTR mice were used. Prior to harvesting retina, one group received a unilateral optic nerve crush whereas the second group was untreated. Retinas from both groups were harvested 7 days post-crush, 1.2 x 10^3 MG cells were isolated from each group and placed *in vitro* in multi-chamber slides. Each set of isolated MG cells were treated once on day 1 with 5ng/mL granulocyte-monocyte colony-stimulating factor (GM/CSF) and 100U/mL interferon gamma (IFN-γ) (Fig. 23A-B). $CD11b^+CD11c^-$ bone marrow cells (BMC), 1.3 x10^4, from CD11c-DTR mice were treated as a control (Fig. 23C-D). Six days post-plating all cells were fixed and stained for CD11b and GFP expression to assess conversion to DC based on GFP expression. No expression of GFP and thus no CD11c-positive cells, were found in either group of MG isolated from retina. In contrast, GM/CSF and IFN-γ treated bone marrow cultures were populated with many GFP^+ cells. Other strategies were done in vivo to analyze if MG are able to differentiate into DC-like cells in retina.

Origin of DC in Retina: Retinal $CD45^+$ Cells Change Phenotype from 45^{hi} to 45^{med} After Bone Marrow Grafting.

It is well established that immune system cells from peripheral blood, as well as in primary and secondary lymphoid tissues, express CD45 at a high level (note Fig. 13)

(75). In contrast, retinal tissue contained two distinct $CD45^{+}$ populations, one with high expression of CD45 ($CD45^{hi}$) and one with medium expression ($CD45^{med}$), (Fig. 12) and the CD11c-DTR-GFP^{+} DC were found in the $CD45^{med}$ population. It is hypothesized that the environment of the retina might play a role in altering the CD45 expression level. To test this hypothesis, CD11c-DTR bone marrow, derived from CD45.2 mice, was grafted into irradiated *wt* B6 CD45.1 mice and examined 1, 2 and 4 weeks after transplantation. If the hypothesis were true, then the expected results would show a reduction in the level of CD45 expression in retina over time, induced by the environment of the retina.

The ratio between $CD45^{med}$ and $CD45^{hi}$ cells changed with time in grafted animals (Fig. 24). In retina of chimeric mice at 1, 2, and 4 weeks post bone marrow grafting, the $CD45^{med}$ population, largely microglia (98%), seemed to be radioresistant relative to the $CD45^{hi}$ population, which was rapidly depleted. One week post-grafting of CD45.1 BM into CD45.2 recipients no chimerism was established in retina, in contrast to peripheral blood (Fig. 24B). Evidence of repopulation of the $CD45^{hi}$ cells from donor bone marrow was observed 2 weeks post-bone marrow grafting in retina as well as in brain. Interestingly, we observed a higher degree of chimerism in brain than in retina at that time point (Fig. 24C), probably representing the contamination of brain with meninges, which would be expected to repopulate quickly. At 4 weeks post-grafting the amount of chimerism between retina and brain were very similar. Very few $CD45^{med}$ donor cells were found in retina, whereas in brain a small population of $CD45^{hi}$ donor cells was found (Fig. 24D). Since all donor cells were recruited from circulating $CD45^{hi}$ cells, the

movement of donor cells into the CD45^{med} population in retina or brain reflects their response to the local environment, which appears to induce the CD45^{med} cells.

Origin of DC in Retina: Optic Nerve Crush Affects Phenotypical Change of Retinal CD45^{+} Cells from 45^{hi} to 45^{med} After Bone Marrow Grafting.

In the CNS, resident MG, and the GFP^{+} DC that were found, express CD45 at an intermediate level, significantly below that of the other cells of the immune system elsewhere in the body (note Figure 13). In the response to an ONC in the CD11c-DTR/GFP mice, the increased number of GFP^{+} cells have the CD45^{med} phenotype as was shown in Figure 24, an observation consistent with an origin in the retina. Using BM chimeras, in which potential local progenitor niches can be depleted, and circulating progenitors can be replaced by progenitors that can be tracked, one can ask if the retinal environment modulates CD45 expression, and seek evidence for a circulating precursor of the GFP^{+} DC that appear in the retinal injury response. The effect of an optic nerve crush on the expression level of CD45 cells was tested in radiation bone marrow chimeras made by grafting CD45.2 CD11c-DTR/GFP bone marrow into lethally-irradiated (12.5 Gy) CD45.1 recipients. The recipients were not head-shielded to allow radiation depletion of local, retina progenitors. In Figure 24, we showed that the CD45^{med} cells in the retina, that did not receive an injury stimulus, were only slowly replaced by donor-derived cells, and that these first appeared in the CD45^{hi} population. The hypothesis is that an optic nerve crush should lead to a faster repopulation of the retinal cells from circulating progenitors, and that it would reveal their modulation of CD45

expression from hi to med by the retinal environment. If this is the case, then the number of $CD45^{med}$ donor-derived cells in retina would be much higher following on optic nerve crush done at 4 - 5 weeks after bone marrow grafting as compared to chimeric mice that did not receive an optic nerve crush. A unilateral optic nerve crush was performed 33 days post-bone marrow grafting. Retinas were harvested 7 days post-optic nerve crush and analyzed for GFP and CD45 expression by FACS. It was found that the optic nerve injury accelerated the MG turnover in the bone marrow chimeras. Further, donor cells were stimulated by the injury to substantially occupy both the $CD45^{med}$ and the $CD45^{hi}$ populations (Fig. 25B,C; Table 4). In the ipsilateral retina, GFP^{+} DC were a large part of the donor population recruited into the retina; recruitment into the contralateral was significant, but less, even though there is no direct injury to the contralateral retinal ganglion cells. The turnover of these populations occurred in a very short time, as retinas were harvested only 7 days post-crush injury. This observation shows that the environment of the retina, post-crush injury, is able to induce the down-regulation of CD45, as all circulating precursors have a high expression of CD45. These results differed from the chimeric mice that did not receive a crush injury, where the majority of resident host cells (MG) was still found in the $CD45^{med}$ compartment (Fig. 24D).

Origin of DC in Retina: Retinal GFP^{+} DC Decreased After B6 Bone Marrow was Grafted into CD11c-DTR Mice.

To further explore the origin of retinal DC bone marrow transplanted chimeric mice were used. CD45.1 bone marrow was grafted into irradiated CD11c-DTR (CD45.2) recipients,

to examine the origin of these cells and their turnover. If the GFP^+ DC were derived from circulating CD11c-DTR progenitors, the GFP^+ DC in the bone marrow chimeras should decline due to the lack of these precursors. If MG were the source of the retinal GFP^+ DC, then one would expect GFP^+ DC to readily repopulate using the surviving CD11c-DTR MG as precursors. The mice were made to be highly chimeric (≥ 95 %), so that few CD11c-DTR precursors remained. Analysis shows that the number of GFP^+ DC steadily declined, and dropped below the average of normal control retina by 43 days post-grafting (Fig. 26). At 77 days post-grafting, the number of GFP^+ DC in all recipients was below the normal range of control retina. The results show that GFP^+DC slowly disappear in uninjured retina of chimeric mice using CD11c-DTR hosts, reaching approximately 25 % of the normal control level after 6 weeks, consistent with a low basal rate of turnover. The two outliers at day 36 are probably due to corneal injuries, which stimulate appearance of the GFP^+ DC in retina.

Since DC numbers steadily declined, MG did not appear to be a source of the GFP^+DC. However, if the precursors were MG, then turnover of the endogenous MG in the chimeras within this time frame could decrease their numbers, reducing the size of the precursor pool. To detect MG turnover, MG were assayed following radiation/bone marrow grafting by flow cytometry for CD45.1 (donor) vs CD45.2 (recipient) cells. At 4 weeks there was little turnover (Fig. 24D), so that replacement of host MG (CD11c-DTR origin) by donor MG was minimal.

To test the possibility that radiation damage to the retina from the chimerism protocol would be sufficient to increase the number of GFP^+ DC, CD11c-DTR mice were subjected to irradiation by one of three protocols: 1) conventional 12 Gy total body irradiation given in divided doses, followed by grafting of C11c-DTR bone marrow; 2) 12 Gy total body irradiation given in divided doses, and additional 6 Gy to the head by lead-shielding the body followed by grafting of C11c-DTR bone marrow; and 3) 18 Gy in divided doses to the head with lead-shielding the body; no bone marrow was transplanted. Retinas were counted for GFP^+ DC at 1, 2, and 5 weeks post-irradiation. None of these procedures resulted in elevated retinal GFP^+ DC counts, even though endogenous circulating precursors were maintained (data not shown). Concerns for radiation damage causing upregulation of GFP^+ DC numbers were not supported by the results.

Origin of Retinal DC: Following Injury, Retinal $CD11c^+$ DC are Recruited from Local Progenitor Cells.

Following injury, it is possible that the origin of retinal DC might be different than in uninjured control retina, as optic nerve crush stimulated a significant increase in the number of GFP^+ DC in the ipsilateral retina, and a smaller increase in the contralateral retina (Fig. 16). To assay for local DC progenitors, bone marrow chimeras were made in CD11c-DTR mice by irradiation and B6 CD45.1 bone marrow grafting. At 62 days post-bone marrow grafting, an optic nerve crush was performed, followed by harvesting on day 69 (Fig. 27 Top). Despite the lack of GFP-labeled circulating precursors, a significant

elevation of GFP^+ DC was found. Assays done on days 42 and 75 show that irradiation alone resulted in only approximately 25 GFP^+ DC in the chimeric retinas prior to injury.

To further control for the number of GFP^+ DC present in the chimeric retinas at the time of injury, a unilateral enucleation was done at 42 or 77 days post-bone marrow grafting. The enucleation includes a unilateral axotomy. The contralateral retina, which displays a sympathetic GFP^+ DC response to the axotomy as observed with the optic nerve crush (Fig. 16), was collected on days 70 and 120, respectively, after the axotomies. The retinas collected at 70 days post-grafting contained an elevated number of GFP^+ DC relative to the ipsilateral controls (Fig. 27 Bottom). The retinas collected at 120 days post-grafting also showed a significant elevation in GFP^+ DC. Based on analysis of blood, the mice were highly (>95%) chimeric with GFP-negative bone marrow. Consequently, these GFP^+ DC came from a non-circulating source. Possible non-circulating sources include MG. Since the previous experiments show no evidence of a MG contribution after crush-injury (Fig. 26), that mechanism is improbable. Another source could be due to the ability of the GFP^+ DC to proliferate. Since DC are not known to be able to expand through the several cycles of division (from 25 cells/retina to 800 cells/retina) their contribution should be minimal (76). The results are most consistent with the activity of local progenitor cells capable of expanding the number of GFP^+ DC.

Origin of Retinal DC: Retinal GFP$^+$ DC can be Depleted with DTx in Grafted and Ungrafted Mice.

The absence of circulating GFP-labeled precursors suggested a local progenitor population that could continue to produce reduced numbers of GFP$^+$ DC in the retinas of CD11c-DTR mice made chimeric with B6 bone marrow. The literature suggests that hematopoietic progenitor cells circulate in small numbers, and replenish myeloid progenitor cells in peripheral niches (77, 78). The local niches in the radiation bone marrow chimeras would be replenished by *wt* B6 hematopoietic progenitor cells, thereby depleting the numbers of GFP$^+$ progenitors over time. Further, stimulation should deplete progenitors in the niches faster due to their limited capacity for self-renewal, and ongoing replacement by donor hematopoietic progenitor cells.

The surviving host-derived, retinal GFP$^+$ precursors in radiation bone marrow chimeras were stimulated by an ipsilateral optic nerve crush and an anterior chamber needle stick. DTx was injected into the anterior chamber to deplete existing GFP$^+$ DC in the 4 groups shown in Fig. 28, represented by the 4 bars under the horizontal axis. Each bar represents the timing of the injury, DTx treatment, and harvest. For example, the first experiment was initiated on day 26 post-bone marrow grafting by an optic nerve crush. The mice were given an anterior chamber injection of DTx on day 36, and harvested on day 40. Three retinas had no GFP$^+$ DC, the fourth had 10. A needle stick injury alone stimulated a GFP$^+$ DC response by day 4 (Fig. 15), and optic nerve crush induced a large DC proliferative response in a CD11c-DTR mouse (Fig. 16). Thus, the absence of a response

after DTx treatment suggests that depletion of the progeny of a local niche, combined with the absence of circulating GFP^+ progenitors able to give GFP^+ DC, left the retina depleted of precursors able to form GFP^+ DC. It also shows that the chimerism protocol employed here effectively eliminates precursors to GFP^+ DC in the host retinas.

However, not all of the GFP^+ DC were depleted. Thus, additional depletion paradigms were employed to see if the local niche could be even more exhausted of precursors. The second group of mice received the first treatment as described, and a second set of treatments including bilateral needlestick injections into the cornea at 45 days, additional bilateral DTx injections into the anterior chamber at 50 days, and harvesting at 55 days. The third group of mice received the second treatment as described, and a third set of treatments including bilateral needle stick injections into the cornea at 60 days, additional bilateral DTx injections into the anterior chamber at 65 days, and harvesting at 70 days. The fourth set included a unilateral optic nerve crush at 83 days, bilateral DTx injections into the anterior chamber at 93 and 98 days, and harvesting at 109 days. The results of these experiments show that depletion of the responding cells by DTx severely reduced subsequent response to injury. This data supports the hypothesis that activity of retinal precursors in a local niche form DC (Fig. 26), and if that niche was exhausted (Fig. 28), no additional GFP^+ DC could be produced in response to the optic nerve crush or needle stick injury. The $CD11b^+$ MG were not depleted by these procedures (data not shown). The potential remained that a small population of circulating cells had survived the irradiation and was able to reconstitute the GFP^+ DC population in the retina. To support

the hypothesis that local precursors exist that can form DC in retina, chimeras were produced where the hosts were CD11c-DTR and the donors were *wt* B6 mice. In order to test whether depletion of host DC would affect the results, DTx was administered prior to the optic nerve crush. If local progenitor cells already expressed the DTR/GFP protein for the transgenic CD11c promoter then no GFP^+ DC would be detected. This experiment also controlled for the circulating survivors of the radiation bone marrow chimeras that might be able to reconstitute, since the anterior chamber injections of 5 ng DTx do not kill $CD11c^+$ cells systemically. The local progenitor cells seemed either to express or rapidly upregulate CD11c, since the retinas of DTx treated eyes showed reduced numbers of GFP^+ DC in their retinas after optic nerve crush at 41 days post-grafting relative to the retinas of the contralateral (untreated) eyes of these mice, which had highly elevated numbers of GFP^+ DC (Fig. 29). If the GFP^+ DC were derived solely from circulating precursors, both eyes should have upregulated GFP^+ DC. Thus, a source for these retinal GFP^+ DC was local progenitor cells.

Origin of Retinal DC: Following Injury, Retinal $CD11c^+$ DC are also Recruited from the Circulation and from Local Progenitor Cells.

The prior experiments support the hypothesis that local progenitor cells contributed to the GFP^+ DC population, and MG did not. The question remained whether there is also recruitment from the circulation. To test this, CD11c-DTR bone marrow was grafted into irradiated *wt* B6 recipients. The mice were >95% chimeric. At 57, 74 or 94 days post-grafting, a unilateral optic nerve crush was performed. The indicated retinas were

harvested at 67, 83 or 103 days, for GFP^+ DC counting. Some mice in the group receiving the optic nerve crush on day 57 were also given an anterior chamber administration of DTx the day prior to harvest (Fig. 30). The contralateral (unmanipulated) retina had low numbers of GFP^+ DC at 85 and 105 days post-grafting at 2 ± 0 (N=1) and 49 ± 3 (N=2), respectively. The ipsilateral optic nerve crush-treated retina had elevated numbers of GFP^+ DC (Fig. 30 and Fig. 31). Recruitment of donor cells into the normal control eyes was modest, even though the retina that is contralateral to an optic nerve crush recruits an elevated number of GFP^+ DC in CD11c-DTR mice. Clearly, the optic nerve injury stimulated recruitment of precursors of GFP^+ DC into the ipsilateral retinas from the circulation and thus, from the transplanted bone marrow.

Origin of Retinal DC: A Model for Regeneration of Retinal GFP^+ DC from a Local Niche of Hematopoietic Progenitor Cells.

Most hypotheses regarding the source of the myeloid cells in the CNS with a perivascular morphology postulate their direct recruitment from circulating monocytes (Fig. 32, path #1). The evidence that GFP^+ DC can be recruited in large numbers to injured retina from donor bone marrow grafts (Fig. 30), demonstrates the DC can be recruited from hematopoietic progenitor cells in the circulation, Additionally, the data also supports a second course for retinal DC (Figs. 26-29) demonstrating that recruitment also includes the participation of progenitor cells of donor origin into retinal niches where they can expand and generate the GFP^+DC from this niche - an indirect route of "recruitment" (Fig. 32, path #2).

Hematopoietic progenitor cells are now well-established to circulate in the circulatory system in normal mice at a low frequency (78), and at a higher frequency in response to inflammation, injury, or cytokines (G-CSF) exposure, all of which stimulate their release from bone marrow. These hematopoietic progenitor cells enter niches in peripheral tissues and give rise to DC locally (77). The continuous, low level of hematopoietic progenitor cell recirculation that is found in normal, untreated mice strongly suggests that maintenance of peripheral niches may be one of their functions (77). Even CNS was shown to implant bone marrow-derived progenitor cells following the *i.v.* inoculation of a bolus of bone marrow-derived stem cells used in the bone marrow grafting procedure (79). Similarly, as shown in the present studies in retina, local progenitor cells, perhaps originally derived from hematopoietic progenitor cells, also appear to implant into a retinal niche.

If retinal niches are a source of the GFP^+ DC, replacement of putative progenitor cells in retinal niches by donor cells in BM chimeras may be incomplete, as retinal GFP^+DC were still found after grafting *wt* BM into CD11c-DTR recipients. Even after 120 days of 95^+ % chimerism with GFP-negative donor cells, an optic nerve crush induced a substantial number of GFP^+ DC in the retinas of these mice (Fig. 27), consistent with survival of host-derived progenitors. At this time it is not possible to distinguish between progenitor cells populating a local retinal niche, from the recruitment of progenitor cells with self-renewal and proliferative capacity from the blood stream (Fig. 32, path #3).

Repopulation of the CD11c-DTR GFP^+ DC in the retina of radiation bone marrow chimeras did not appear to be due to cellular influx caused by radiation damage to the brain/retina, as even 18 Gy exposure of the head, with body shielding, did not induce a GFP^+ DC injury response in the retina. I propose that a small number of hematopoietic progenitor cells normally occupy a specific niche in the retina, and that the irradiation depletes that niche, providing space for new, replacement hematopoietic progenitor cells that can be derived from exogenous, transferred hematopoietic progenitor cells. Such niches may be limited, fully occupied under normal circumstances, and subject to only minimal turnover in the absence of a stimulus, very much like the bone marrow niche for hematopoietic stem cells (80). A niche populated by progenitors with limited capacity for self-renewal in normal retina would appear to be depleted by stimulation, leaving niche space available to circulating progenitors. The optic nerve crush-injury may promote engraftment of hematopoietic progenitor cells into retina and stimulate production of donor progeny in chimeric mice.

Figure 6. Wholemount retina.

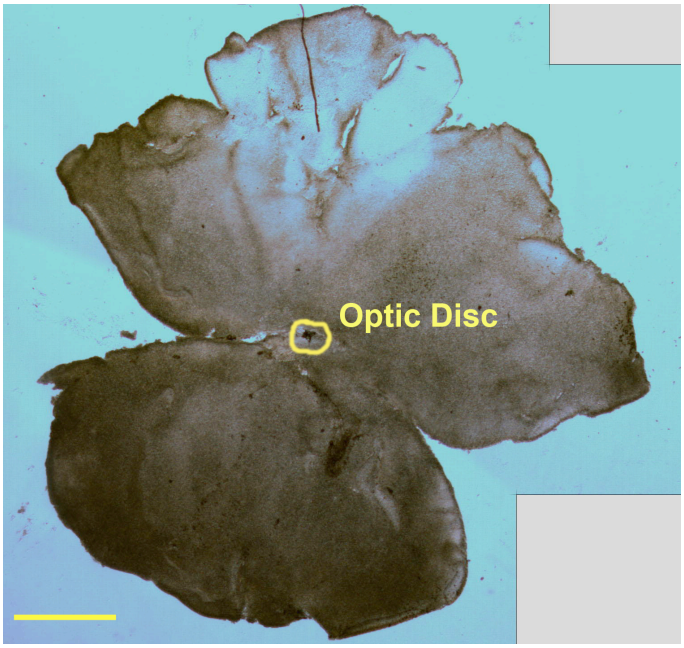

Figure 6. Wholemount retina. A flat mount of the whole murine retina is approximately 3 mm in width and 175 microns thick. Scale bar, 500 μm.

Figure 7. Distribution of GFP$^+$ cells in quiescent retina from CD11c-DTR mice.

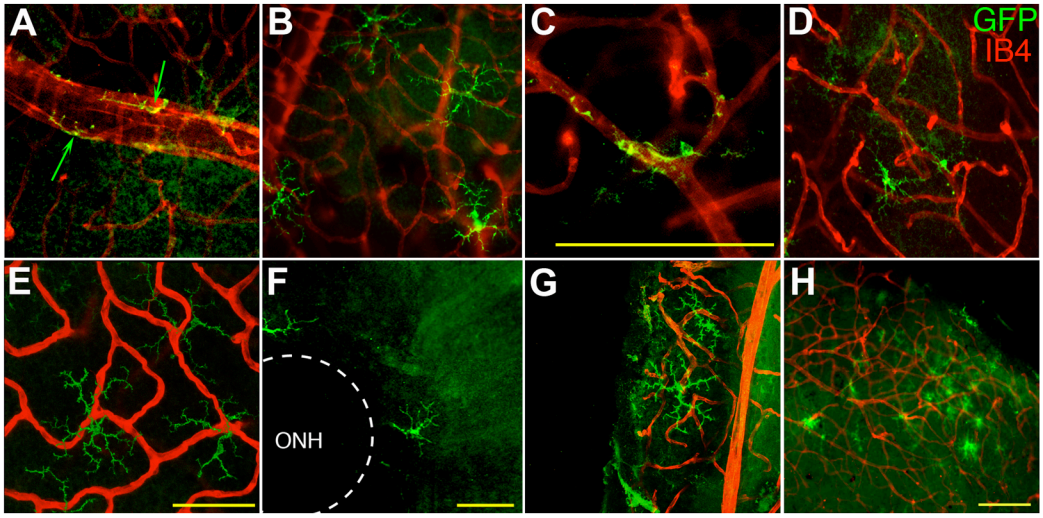

Figure 7. Distribution of GFP^+ cells in quiescent retina from CD11c-DTR mice. GFP^+ cells (green) were detected with AF488-labeled anti-GFP; blood vessels (red) were stained with AF594-labeled isolectin B_4 (IB4). GFP^+ cells in the GCL were found to exhibit either a highly elongated perivascular cell morphology with large blood vessels (A, arrows)**,** or a highly ramified morphology (B). A few GFP^+ cells in the GCL were associated with branch points in smaller blood vessels (C). GFP^+ cells in the IPL (D) and OPL (E) were also highly ramified. Examination of the lateral distribution of the GFP^+ cells showed cells that were close to the optic nerve head (ONH) (F) or in the far periphery (G). Occasional clusters of GFP^+ cells were found in the same focal plane as the extensively branched network of blood vessels near the surface of the retina (H). Scale bars, 50 μm (A - G), or 100 μm (H).

Figure 8. Hematoxylin and eosin stain of a cross-section through a murine retina.

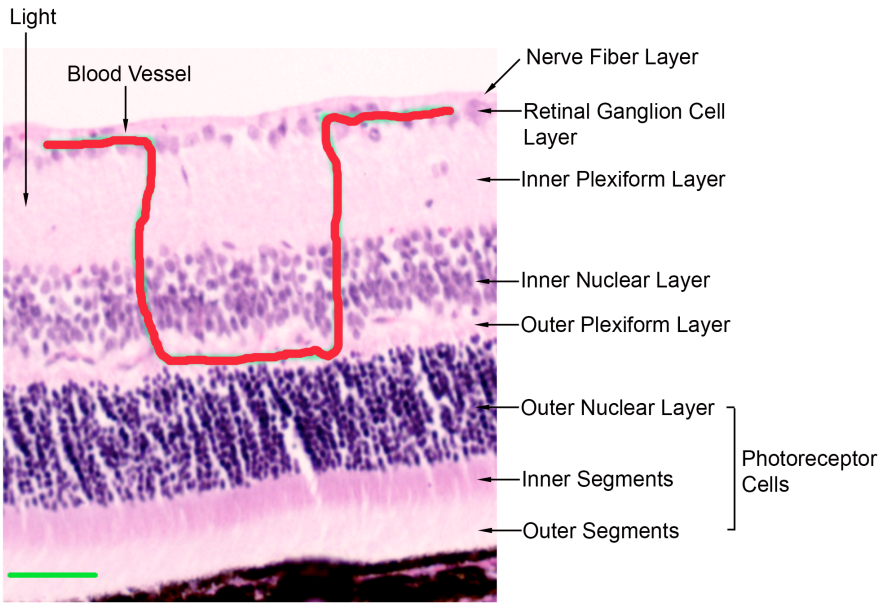

Figure 8. Hematoxylin and eosin stain of a cross-section through a murine retina.

Scale bar, 50 μm.

Figure 9. Side view of the ramified GFP^+ DC from Figure 7E.

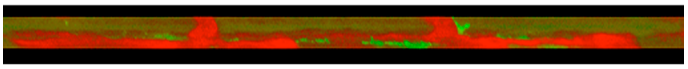

Figure 9. Side view of the ramified GFP$^+$ DC from Figure 7E. Retina from a CD11c-DTR mouse was stained with anti-GFP (green, CD11c$^+$ DC) and isolectin B_4 (IB4, red, blood vessels). The confocal images were stacked to give a 12 μm thick section. The extensive dendritic processes of these cells were limited to this section of the OPL.

Figure 10. Stratification of the CD11b^{+} (green) cells, which include DC and MG, in the quiescent retina.

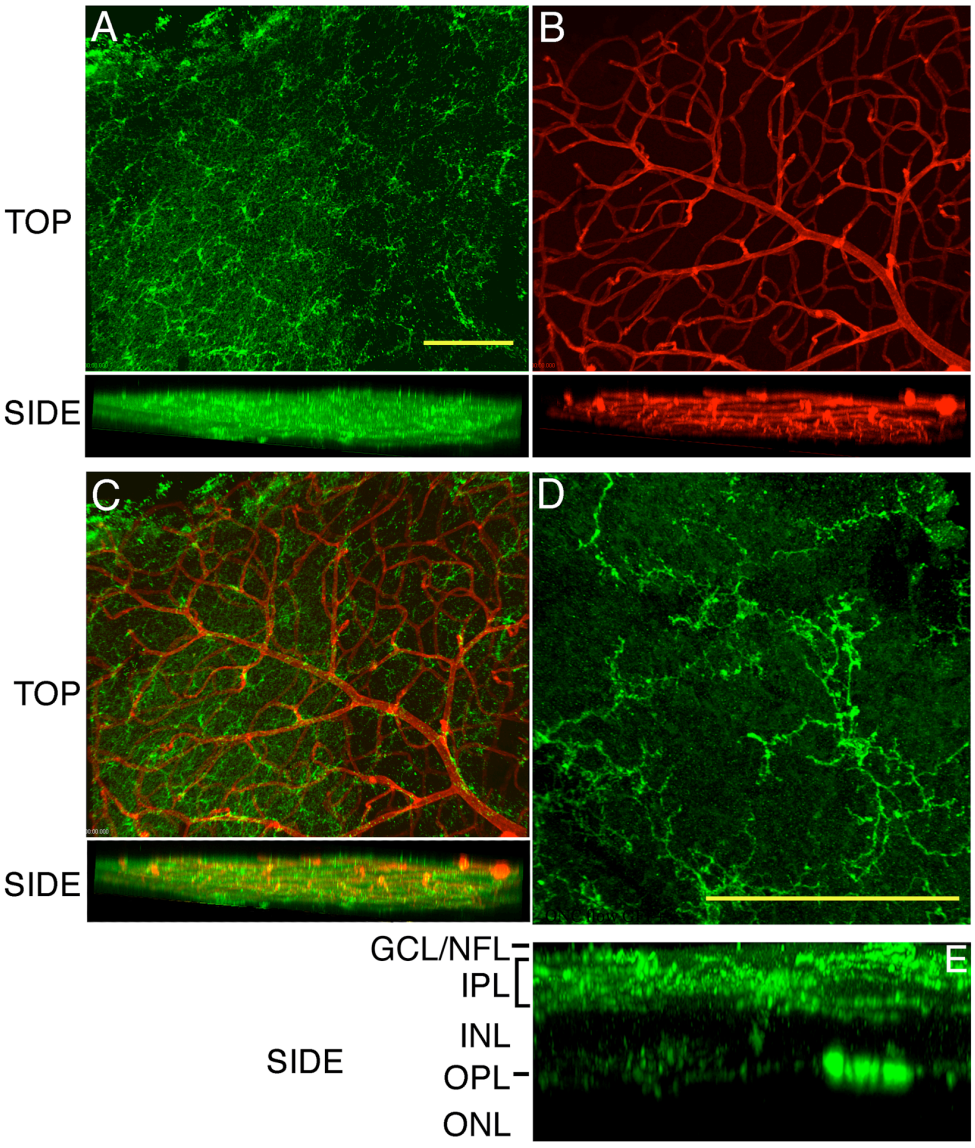

Figure 10. Stratification of the CD11b$^+$ (green) cells, which include DC and MG, in the quiescent retina. (A, B) Most of the CD11b-labeled cells in this flatmount (panel A, top view) were found intermingled with the highly branched layer of blood vessels (IB4$^+$) in (panel B, top view, red) in the innermost 40 – 50 microns of the retina. (C) Panels A and B merged. (D) High magnification image of CD11b$^+$ cells. (E) Side view of panel D, showing a less dense population of CD11b$^+$ cells in the OPL. Scale bars, 50 μm.

Figure. 11. Retinal GFP$^+$ DC in quiescent retina also express CD11b$^+$ and MHC class II.

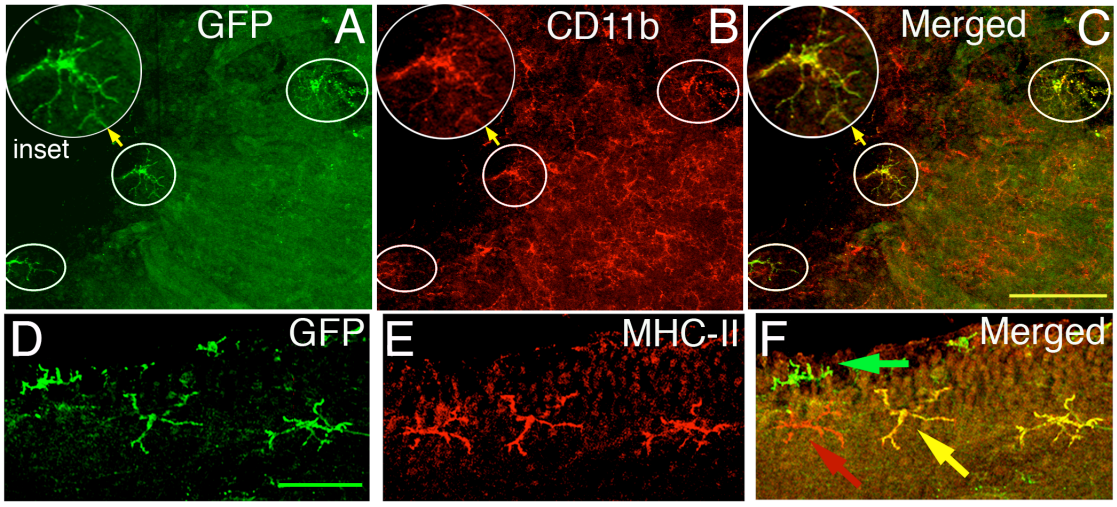

Figure. 11. Retinal GFP$^+$ DC in quiescent retina also express CD11b$^+$ and MHC class II. (A-C) Area of CD11c-DTR retina near the optic nerve head stained with anti-GFP antibody (A) and CD11b (B). Circled cells are the GFP$^+$ cells from panel A. (C) Merge of A and B showing that all GFP$^+$ cells expressed CD11b, but most CD11b$^+$ cells were GFP$^-$. (D-F) Double staining for GFP$^+$ and MHC class II$^+$ cells in the naïve CD11c-DTR retina. Not all GFP$^+$ DC are MHC class II positive. Scale bars, 100 μm (A-C), or 50 μm (D-F).

Table 1. **Upregulation of MHC Class II on the GFP$^+$ DC by an optic nerve crush.**

	Dendritic Cells		Microglia
Retina	GFP$^+$MHC-II$^+$	GFP$^+$MHC-II$^-$	GFP$^-$MHC-II$^+$
Naïve	4.4%	95.5%	0.2%
ONC injured[a]	49.6%	50.4%	<0.1%

[a]Seven days post-ONC.

Figure 12. The retinal CD45^{med} population contains the GFP^{+}CD11c^{+} cells.

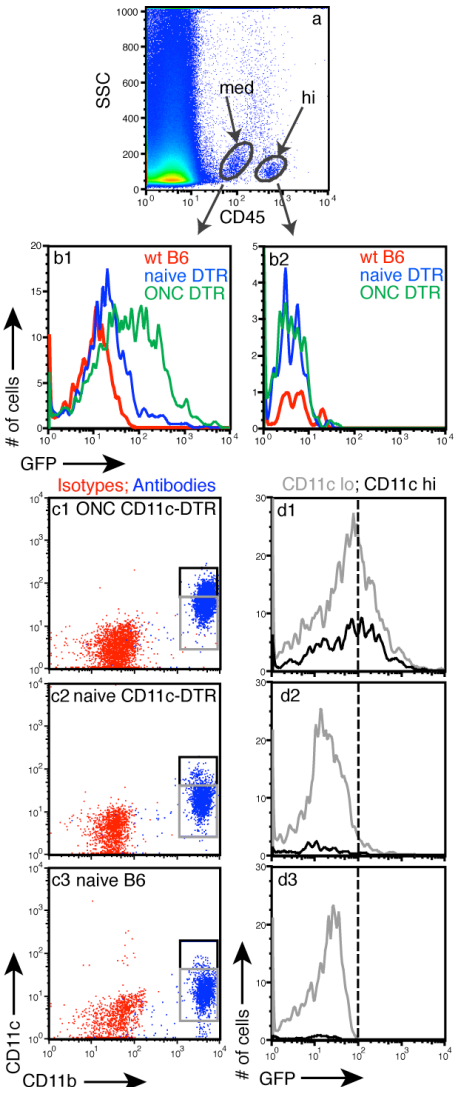

Figure 12. The retinal CD45^{med} population contains the GFP^{+}CD11c^{+} cells. (A) FACS analysis of retinal cell suspensions showing distinct CD45^{+} populations. (B1 and B2) GFP expression in the CD45^{med} and CD45^{hi} populations from retinas of CD11c-DTR mice (blue), control B6 mice (red), and CD11c-DTR mice 7 d following an optic nerve crush (green). (C) FACS analysis of the CD45^{med} population for CD11b and CD11c from the indicated mice. (D) Analysis of GFP levels in the CD11b^{+}CD11c^{lo} (gray box) and CD11b^{+}CD11c^{hi} (black box) populations.

Figure 13. The CD45^{hi} cell population in spleen contains GFP^{+}CD11c^{+} cells.

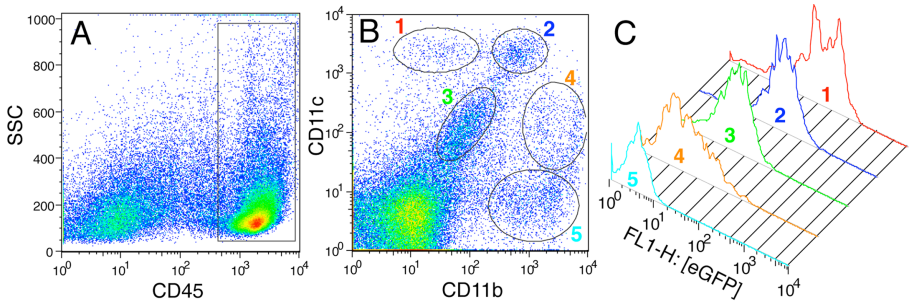

Figure 13. The CD45^{hi} cell population in spleen contains GFP^{+}CD11c^{+} cells. (A) FACS analysis of a CD11c-DTR splenic cell suspension. The CD45^{hi} cells are indicated. (B) Analysis of the CD45^{hi} population for CD11b and CD11c. (C) GFP expression levels in the five populations designated in B.

Figure 14. Hematoxylin and eosin stain of a cross-section through a murine eye.

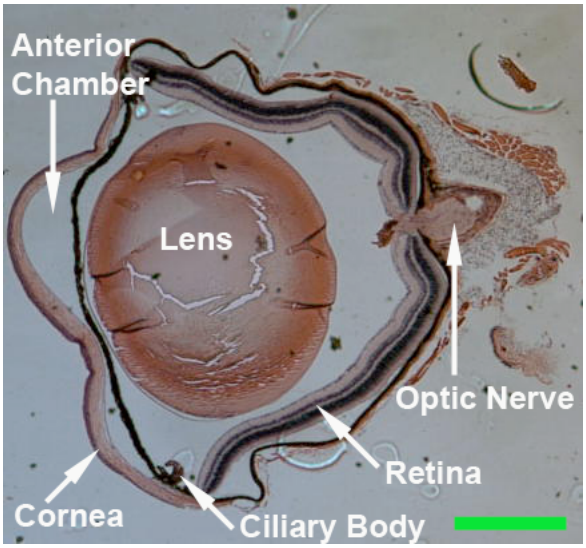

Figure 14. Hematoxylin and eosin stain of a cross-section through a murine eye.

Sections were 7 microns thick. Scale bar, 1000 μm.

Figure 15. Injection of DTx or saline into the anterior chamber induces a response in the retinal GFP$^+$ cells.

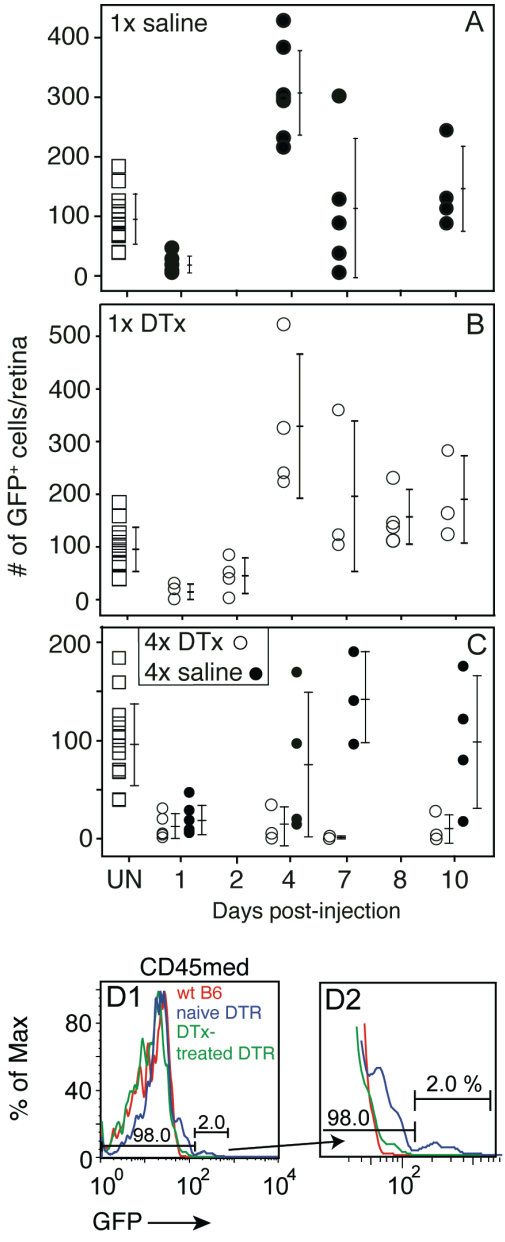

Figure 15. Injection of DTx or saline into the anterior chamber induces a response in the retinal GFP$^+$ cells. (A) A needlestick and injection of 1 ml saline into the anterior chamber is sufficient to induce a flux in the number of retinal DC (N=4-6 per time point). (B) A single injection of 1 ng DTx into the anterior chamber does not result in DC depletion in the retina of the transgenic mice (N=3-4 per time point). (C) Four serial intraocular DTx treatments (1 ng each) depleted the retinal DC (N=3-4 per time point). UN – untreated normal controls. (D1) Flow cytometry following two anterior chamber injections of DTx showed depletion of the GFP^{hi} cells from the retina. Mice were injected on days 0 and 2, and retinas harvested on day 4. (D2) Enlargement of profile showing detail of the DTx-depleted and control populations.

Figure 16. Redistribution and morphological changes in retinal CD11c^{+} cells after an optic nerve crush of CD11c-DTR mice.

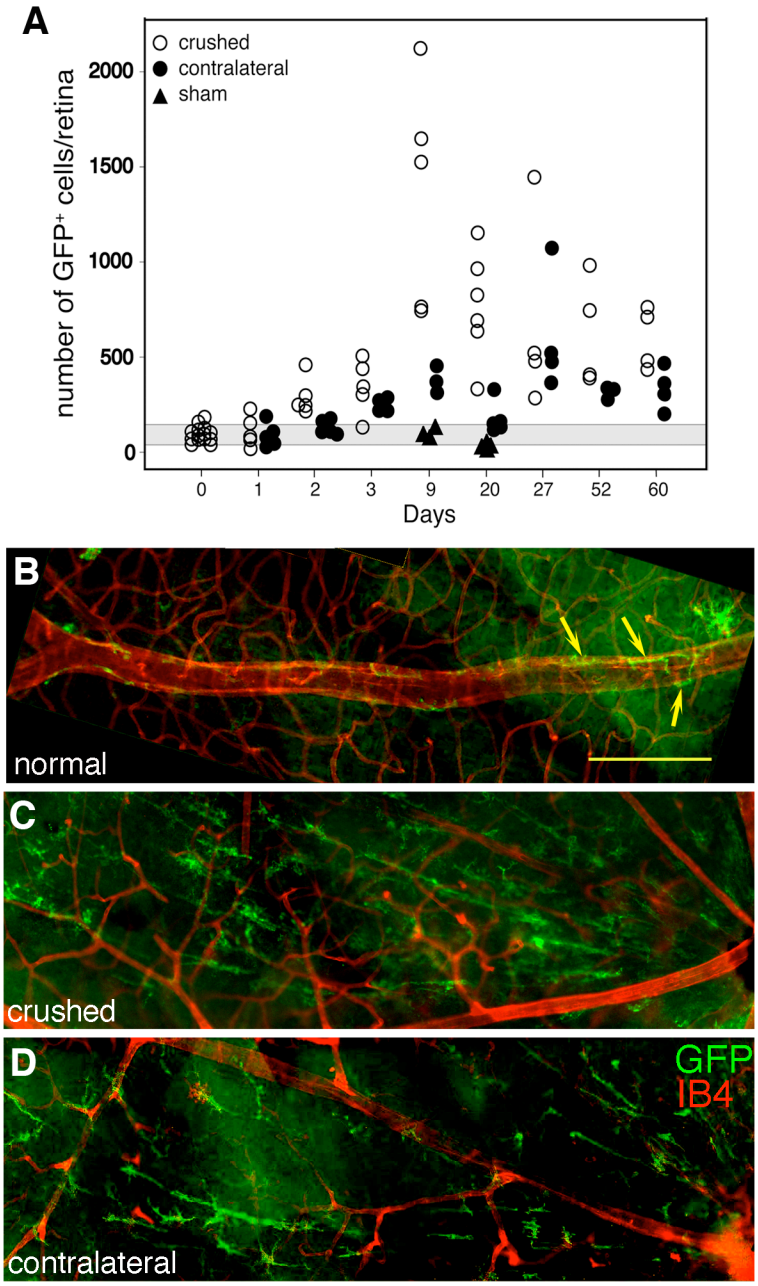

Figure 16. Redistribution and morphological changes in retinal CD11c$^+$ cells after an optic nerve crush of CD11c-DTR mice. (A) Numbers of GFP$^+$ DC in retinas in the crushed (ipsilateral) and uncrushed (contralateral) retinas of optic nerve crushed-mice and in sham-operated control mice. The gray area represents the mean ± 1 SD of the number of GFP$^+$ DC in unmanipulated control mice. (B) Normal retina. Arrows point to GFP$^+$ DC tightly aligned with the large blood vessel (IB4, red). A single ramified GFP$^+$ DC is visible (upper right). (C) Ipsilateral retina 24 days post-optic nerve crush showing elongated, radial orientation of the GFP$^+$ cells. (D) The contralateral retina showing a similar radial arrangement of GFP$^+$ DC, but to a lesser degree. The optic nerve head is on the right in all panels. Scale bar, 100 μm.

Figure 17. GFP$^+$ DC were found tightly associated with nerve fibers after an optic nerve crush-injury to CD11c-DTR mice.

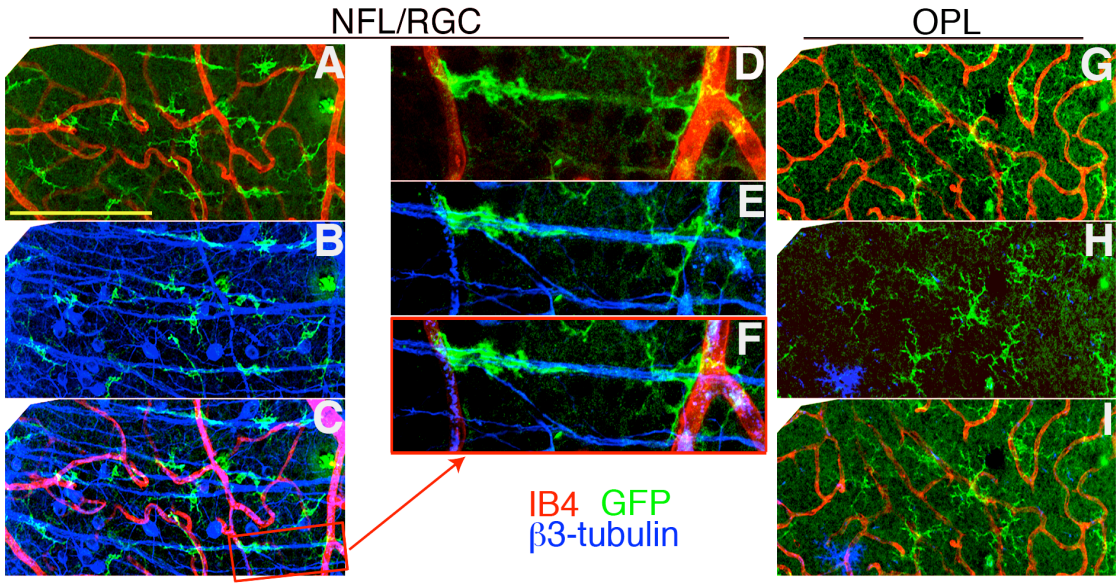

Figure 17. GFP$^+$ DC were found tightly associated with nerve fibers after an optic nerve crush-injury to CD11c-DTR mice. (A-C) A three micron thick retinal section of the NFL/GCL 10 days post-optic nerve crush stained for (A) GFP$^+$ cells (green) and blood vessels (IB4, red), (B) GFP$^+$ cells and nerve fibers (β3-tubulin; blue). (C) Merged image of A and B. (D-F) A higher magnification of the boxed area in image C is shown. (G-I) Confocal stack of the OPL from the same field shown in A-C. Scale bars, 100 μm (A-C, G-I).

Figure 18. The majority of the cells associated with nerve fibers are $GFP^{+}CD11b^{+}$.

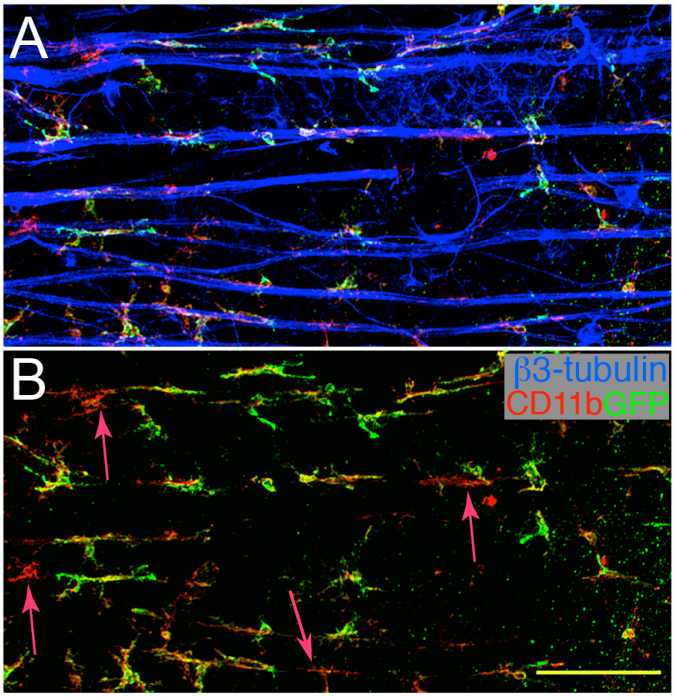

Figure 18. The majority of the cells associated with nerve fibers are GFP^+CD11b^+. (A) A three micron thick optical section of the NFL/RGC from a CD11c-DTR mouse 7 days post-optic nerve crush immunostained for GFP^+ cells (green), $CD11b^+$ cells (red), and nerve fibers (blue). (B) Same field as A analyzed for GFP^+CD11b^+ cells showing very few GFP^-CD11b^+ cells. Red arrows mark the four cells near nerve fibers that were $CD11b^+$ but GFP^-. Scale bar, 100 μm.

Figure 19. Depletion of CD11c^{+} DC with DTx. (A, B) DTx effect on GFP^{+} cells in quiescent retina.

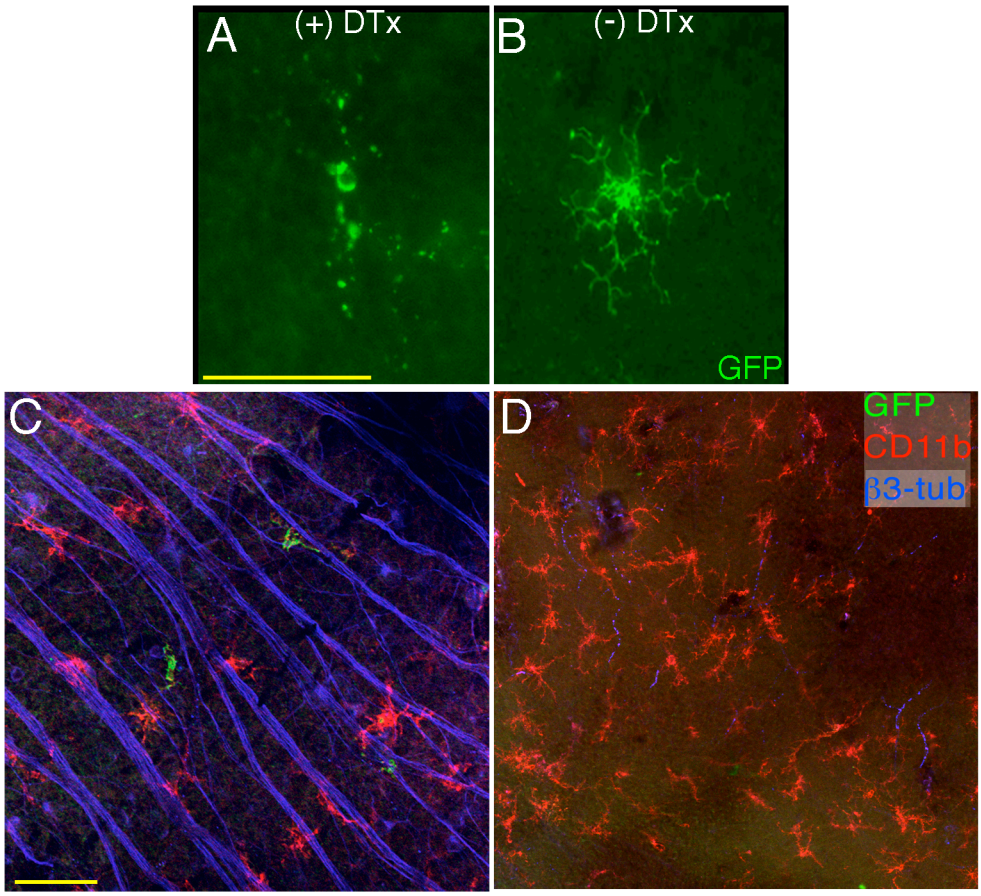

Figure 19. Depletion of CD11c$^+$ DC with DTx. (A, B) DTx effect on GFP$^+$ cells in quiescent retina. (A) DTx (5 ng) was injected into the anterior chamber 18 h prior to harvest. Remnants of a degenerated cell are seen. (B) Untreated GFP$^+$ DC. (C, D) GFP$^+$ DC that respond to an optic nerve crush were toxin sensitive, but MG were not. (C) A three micron thick optical section of the NFL from a CD11c-DTR mouse 7 days post-optic nerve crush immunostained for GFP (green), CD11b (red), and β3-tubulin (blue). DTx (5 ng) was injected into the anterior chamber 31 hr prior to harvest. (D) A 28 micron thick confocal image stack from the IPL showing that the CD11b$^+$GFP$^-$ MG were intact. Scale bars, 50 μm (A, B) and 100 μm (C, D).

Table 2. DTx Treatment Reduces Retinal CD11c$^+$, but not CD11b$^+$, Cell Numbers.

	Naïve	ONC and DTx treated	P value[a]
CD11b$^+$ cells	4291 ± 545 (n = 8)	3971 ± 627 (n = 7)	= 0.58
CD11c$^+$ cells	95 ± 42 (n = 14)	14 ± 14 (n = 4)[b]	< 0.005

[a]T-test comparing cells counts of naïve vs. optic nerve crush/DTx-treated retinas.

[b]Without DTx treatment, 597 ± 163 GFP$^+$ cells were found.

Table 3. **Upregulation of GFP$^+$ DC in the OPL by Exposure to Bright Light.**

	Treatment		
GFP$^+$ DC counts	Control[a]	Light-treated[b]	P value[c]
Total / retina	95 ± 42	614 ± 90	< 0.001
Inner retina (GCL, IPL, INL)	38 ± 17	94 ± 14	< 0.001
OPL	57 ± 25	519 ± 75	< 0.001
Number of retinas	14	7	

[a]Conventional light/dark housing.

[b]Four days continuous light followed by 3 days conventional light/dark cycle, then harvest.

[c]Control vs. light-treated retinas.

Figure 20. Light injury causes a change in the distribution and number of GFP$^+$ DC.

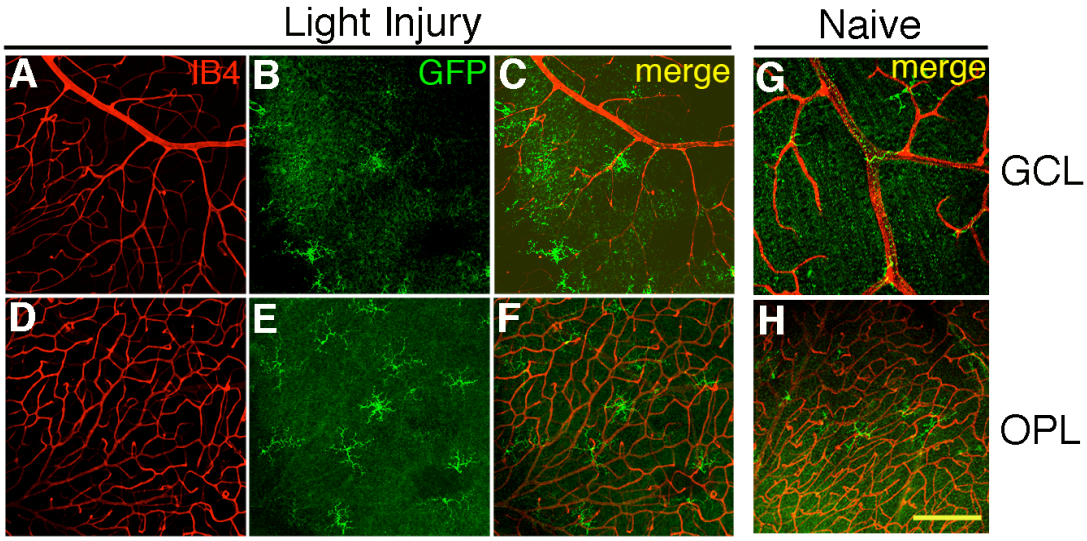

Figure 20. Light injury causes a change in the distribution and number of GFP^+ DC. (A-C) Optical sections from the GCL. (D-F) Same image field as in A-C, but the optical sections were taken from the OPL. (A, D) Blood vessels stained with IB4 (red). (B, E) GFP^+ DC (green). (C, F) Merged. (G) GFP^+ DC in the GCL of naive retinas. (H) OPL from the same field as G. Scale bar, 50 μm. Cell counts are shown in Table 3.

Figure 21. Double immunostaining for GFP$^+$ and MHC class II$^+$ cells in the optic nerve crush-injured CD11c-DTR retina.

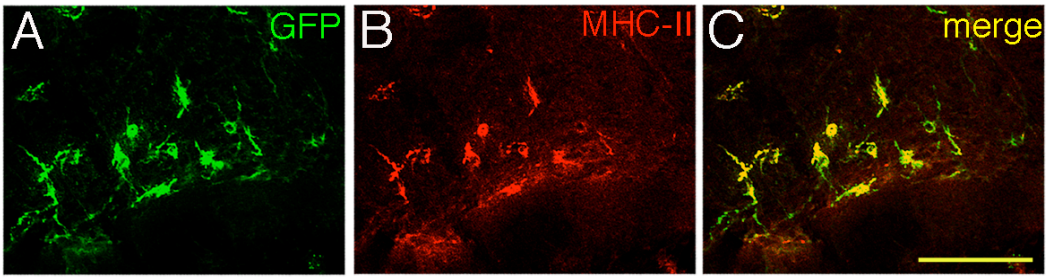

Figure 21. Double immunostaining for GFP^+ and MHC class II^+ cells in the optic nerve crush-injured CD11c-DTR retina. (A) GFP^+ cells, (B) MHC class II^+ cells, (C) A and B merged. In contrast to naïve retina (Fig. 11D-F), the MHC class II^+ cells are also GFP^+ after an optic nerve crush. Scale bar, 100 μm.

Figure 22. Retinal GFP$^+$ DC can activate naïve CD4$^+$ T cells after optic nerve injury.

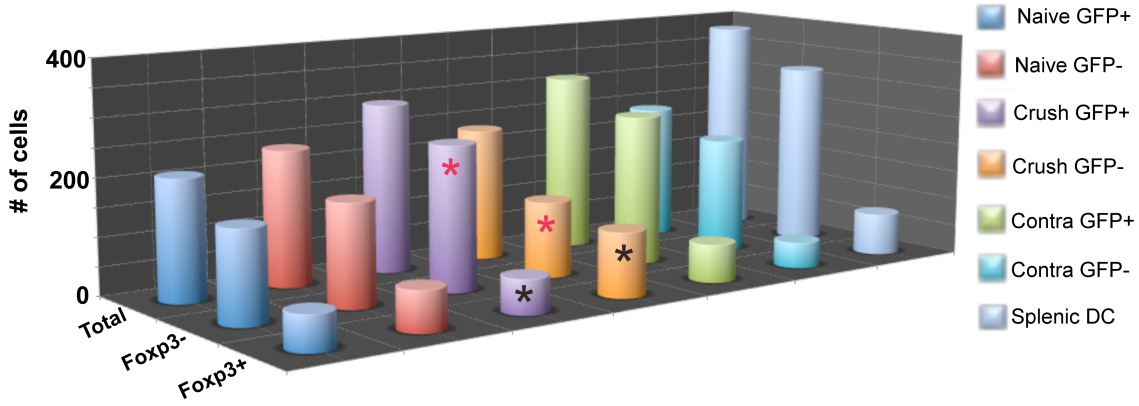

Figure 22. Retinal GFP^+ DC can activate naïve $CD4^+$ T cells after optic nerve injury. Retinas from CD11c-DTR mice were collected from mice that were untreated or had received a unilateral optic nerve crush 7 days prior to harvest. Retinal GFP^+ DC were co-cultured for 4 days with naïve BG2 CD4 T cells, expressing the βgal-specific TCR and GFP under the Foxp3 promoter, βgal peptide, and IL-2. Activated T cells are labeled as $Foxp3^-$ cells and T regulatory cells as $Foxp3^+$ cells. GFP^+ DC from retinas, treated with an optic nerve crush, are the most potent population of retinal cells to activate T cells as compared to the GFP^- population from the same retina, $P<0.001$ (red asterisks). The GFP^- population of cells in the crushed retinas did not activate T cells well, instead it was most potent in the generation of T regulatory cells, $P<0.001$ (black asterisks). The data was analyzed using a paired ANOVA test.

Figure 23. Retinal MG are unable to differentiate into DC-like cells *in vitro*.

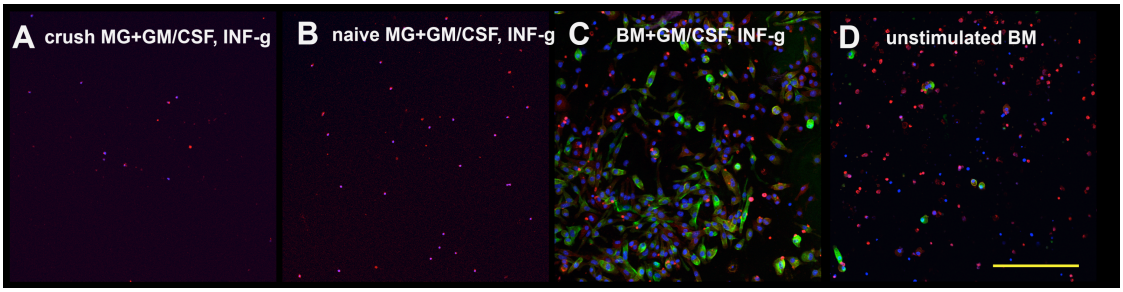

Figure 23. Retinal MG are unable to differentiate into DC-like cells *in vitro*. MG, from mice receiving optic nerve crush (A) or unstimulated (B) were treated with granulocyte-monocyte colony-stimulating factor (GM/CSF) and interferon gamma (INF-γ). Bone marrow, treated with GM/CSF and INF-γ (C) or unstimulated (D), was used as control. All conditions were stained for DAPI (blue), CD11b (red), and GFP (green) 6 days post-treatment. Scale bar, 100 μm.

Figure 24. Radiation bone marrow chimeras reveal the influx of CD45^{hi} donor-derived cells into retina and brain.

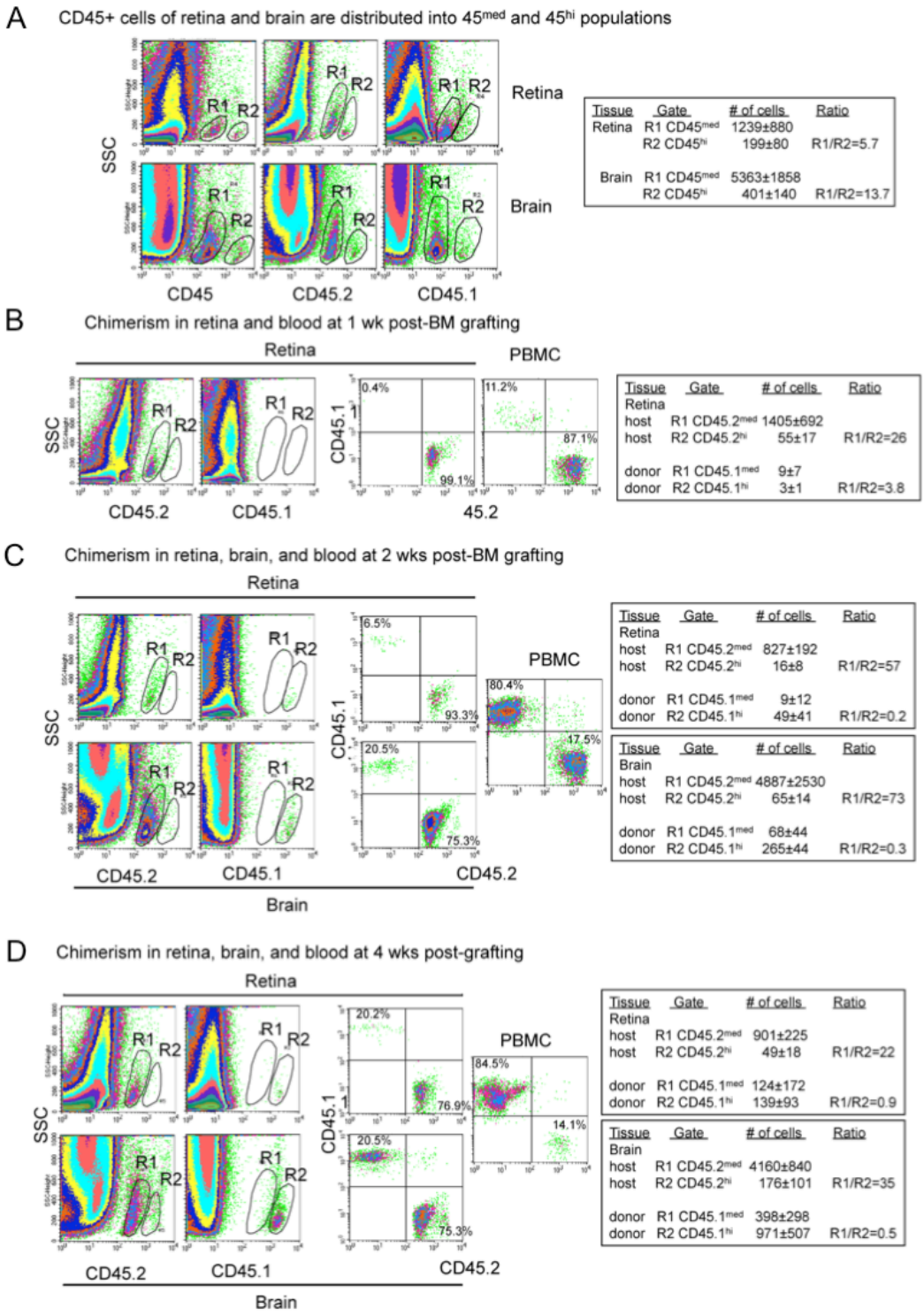

Figure 24. Radiation bone marrow chimeras reveal the influx of CD45^{hi} donor-derived cells into retina and brain. (A) CD45^{+} cells of retina and brain were distributed into CD45^{med} (R1) and CD45^{hi} (R2) populations. (B) One week post-bone marrow grafting of CD45.1 bone marrow into CD45.2 recipients, no chimerism was established in retina but donor cells were apparent in peripheral blood. (C) Two weeks post-grafting, repopulation of CD45^{hi} cells from donor bone marrow was observed in retina and to a higher degree in brain. Blood was highly chimeric. (D) Four weeks post-grafting the level of chimerism in retina and brain were similar, but both lagged well behind the peripheral blood mononuclear cells (PBMC). The vast majority of donor cells in retina and brain remained in the CD45.1^{hi} population.

Figure 25. Optic nerve injury affects turnover of MG in radiation bone marrow chimeras.

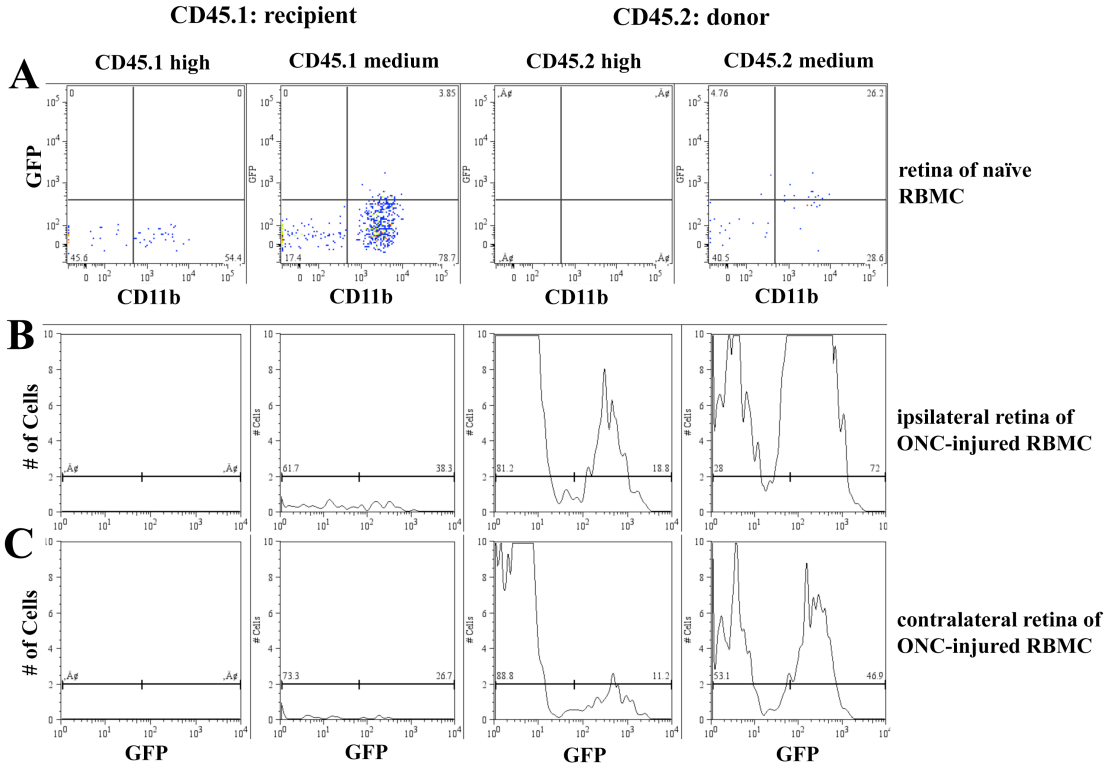

Figure 25. Optic nerve injury affects turnover of MG in radiation bone marrow chimeras. B6 Ly5.1 hosts were irradiated and received bone marrow from CD11c-DTR Ly5.2 mice. Some mice received a unilateral optic nerve crush 7 days prior to harvesting retinas at day 40 post-grafting. (A) Mice, receiving no optic nerve crush, are characterized by a higher number of remaining host MG ($CD45.1^{med}$) and a low number of donor cells ($CD45.2^{med}$ and $CD45.2^{hi}$). Only a few GFP^{+} cells are seen in the $CD45.2^{med}$ population. (B) The ipsilateral retina (received optic nerve crush) of a chimeric mouse shows not only high numbers of donor cells in the $CD45.2^{med}$ and $CD45.2^{hi}$ compartments but it also characterized by many GFP^{+} cells in these populations. (C) The contralateral retina of mouse from B shows a similar pattern, but fewer cells, relative to the ipsilateral retina.

Table 4. Recovery of CD45^{med} and CD45^{hi} cells from retinas of radiation bone marrow chimeric mice after unilateral optic nerve crush.

45.1^{hi}		**45.1^{med}**		**45.2^{hi}**		**45.2^{med}**		CD45.1: recipient
GFP$^-$	**GFP$^+$**	**GFP$^-$**	**GFP$^+$**	**GFP$^-$**	**GFP$^+$**	**GFP$^-$**	**GFP$^+$**	CD45.2: donor
16	0	270	1	3	2	19	12	BM chimeras
5	0	104	12	950	186	394	434	ONC ipsi average
2	0	148	16	420	152	206	138	ONC contra average

Figure 26. The GFP$^+$ DC in the retina decreases after B6 bone marrow was grafted into irradiated CD11c-DTR mice.

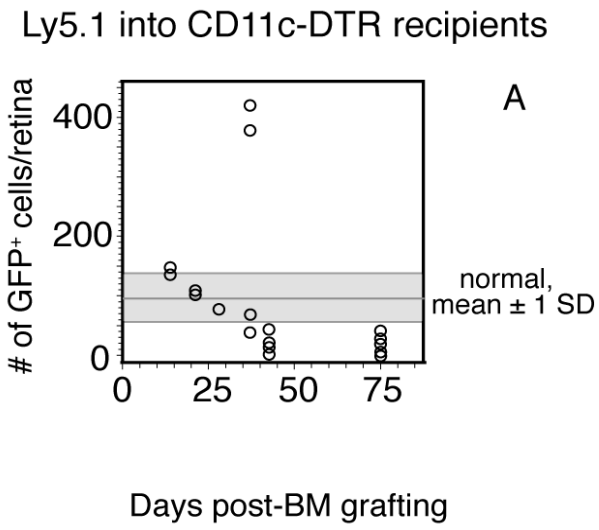

Figure 26. The GFP^+ DC in the retina decreases after B6 bone marrow was grafted into irradiated CD11c-DTR mice. The number of GFP^+ DC in graft recipients that did not receive a retinal stimulus dropped below the normal range by 35 and 43 days post-grafting in 7 of 9 recipients, showing little GFP^+ DC turnover.

Figure 27. Retinal injury stimulates the appearance of GFP$^+$ DC in bone marrow chimeras in which wt bone marrow was grafted into irradiated CD11c-DTR mice.

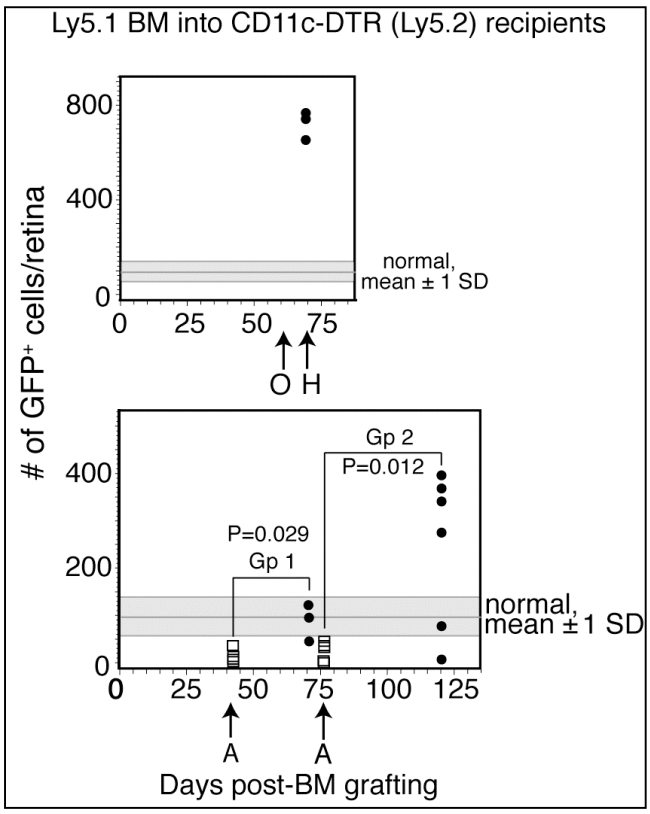

Figure 27. Retinal injury stimulates the appearance of GFP^+ DC in bone marrow chimeras in which wt bone marrow was grafted into irradiated CD11c-DTR mice. (Top) Chimeric mice were given an ipsilateral optic nerve crush to stimulate the appearance of retinal GFP^+ DC. Samples are from ipsilateral eyes after an optic nerve crush (closed circles). Counts from uninjured chimeric mice on day 75 post-grafting are 30 ± 23 GFP^+ DC/retina. (Bottom) Chimeric mice were given a contralateral axotomy to promote the appearance of retinal GFP^+ DC. Samples from injured recipients are from contralateral eyes after an axotomy (solid circles). Control eyes from the radiation bone marrow chimeras are shown in the open squares.

Figure 28. B6 bone marrow was grafted into irradiated CD11c-DTR mice that were then injured to stimulate appearance of GFP$^+$ DC.

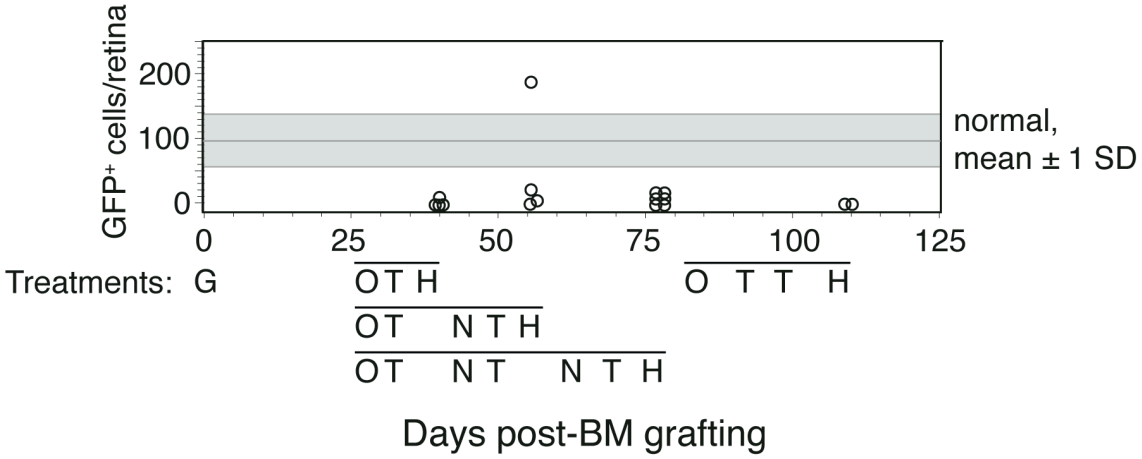

Figure 28. B6 bone marrow was grafted into irradiated CD11c-DTR mice that were then injured to stimulate appearance of GFP^+ DC. Some mice were given DTx treatments to deplete GFP^+ DC. Four sets of treatments were done to stimulate/deplete the GFP^+ DC. The first set included a unilateral optic nerve crush at 26 days, bilateral DTx injections into the anterior chamber at 36 days, and harvesting at 40 days. The second group of mice received the first treatment as described, and a second set of treatments including bilateral needlestick injections into the cornea at 45 days, additional bilateral DTx injections into the anterior chamber at 50 days, and harvesting at 55 days. The third group of mice received the second treatment as described, and a third set of treatments including bilateral needle stick injections into the cornea at 60 days, additional bilateral DTx injections into the anterior chamber at 65 days, and harvesting at 70 days. The fourth set included a unilateral optic nerve crush at 83 days, bilateral DTx injections into the anterior chamber at 93 and 98 days, and harvesting at 109 days. (O) optic nerve crush; (T) diphtheria toxin injection; (N) needle stick; (H) harvest.

Figure 29. B6 bone marrow was grafted into irradiated CD11c-DTR mice that were then injured to stimulate appearance of GFP$^+$ DC.

Figure 29. B6 bone marrow was grafted into irradiated CD11c-DTR mice that were then injured to stimulate appearance of GFP^+ DC. All mice were given unilateral ocular DTx treatments to stimulate/deplete GFP^+ DC. The experimental paradigm involved two DTx treatments at 27 and 29 days, a unilateral optic nerve crush at 34 days, and harvesting at 41 days.

Figure 30. Circulating precursors derived from GFP$^+$ bone marrow grafts (CD11c-DTR donor) did not populate retina of normal mice with GFP$^+$ DC without a stimulus (optic nerve crush), but efficiently occupied retina after the optic nerve crush-injury.

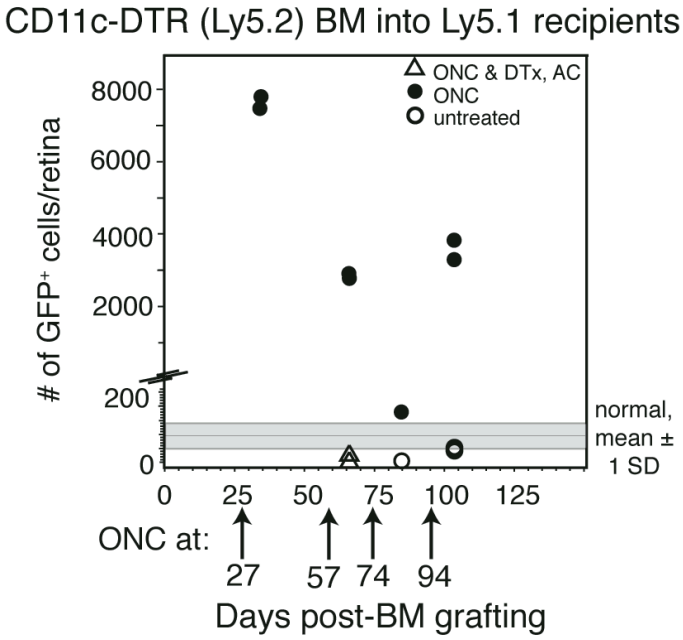

Figure 30. Circulating precursors derived from GFP^+ bone marrow grafts (CD11c-DTR donor) did not populate retina of normal mice with GFP^+ DC without a stimulus (optic nerve crush), but efficiently occupied retina after the optic nerve crush-injury. Unilateral optic nerve crush were performed at 27, 57, 74 or 94 days post-grafting. Retinas were harvested at 36, 67, 83 and 103 days, respectively.

Figure 31. The distribution of GFP$^+$ DC in a chimeric mouse after optic nerve crush.

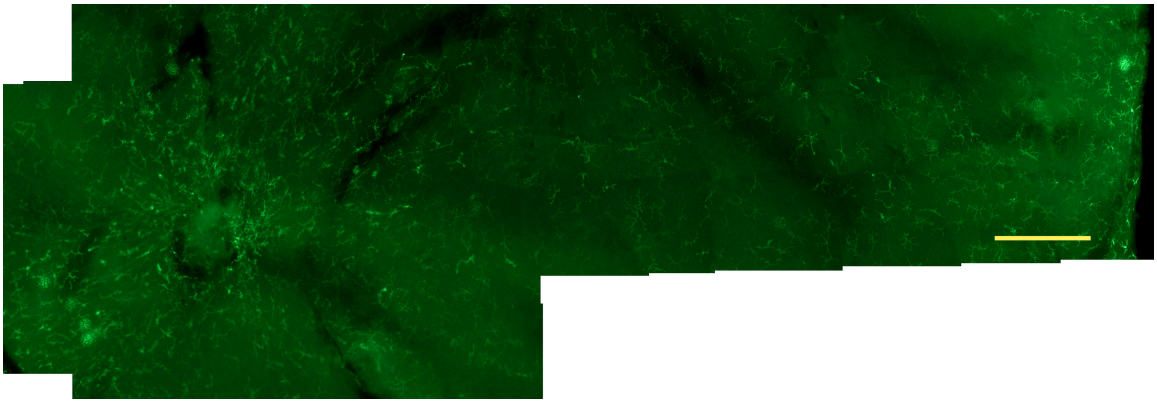

Figure 31. The distribution of GFP^+ DC in a chimeric mouse after optic nerve crush. CD11c-DTR bone marrow was grafted into irradiated *wt* B6 recipients. The mice received an optic nerve crush 57 d post-grafting, and retinas were harvested 67 days post-grafting. Scale bar, 200 μm.

Figure 32. Pathways for the possible origins of retinal GFP$^+$ DC via circulating myeloid precursors.

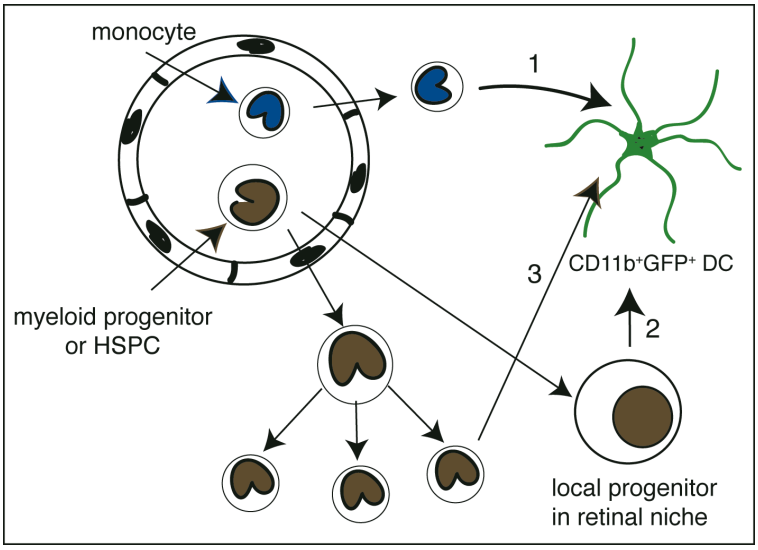

Figure 32. Pathways for the possible origins of retinal GFP$^+$ DC via circulating myeloid precursors. Direct pathways 1 and 3 do not cycle through the proposed local niche. Progenitor cells may stock the niche, providing precursor cells.

DISCUSSION

The presence of DC in retina, particularly normal uninjured retina, has been a subject of controversy. The identification has been hampered by inadequate tools to distinguish between different myeloid cell types, as morphology alone is insufficient to distinguish DC from resident MG, as are markers of the myeloid lineage. The results demonstrate that there is a population of $CD11b^+$ cells that also express CD11c, identified by GFP expression in the CD11c-DTR/GFP transgenic mouse. These GFP^+CD11b^+ DC upregulated MHC class II when stimulated by a retinal injury, in contrast to MG, which expressed little MHC class II. These results, and those which follow below, demonstrate that there are DC in retina distinct from MG. These DC responded rapidly to two different retinal injuries: a crush injury to the axons of retinal ganglion cells in the optic nerve, and light-induced injury to the photoreceptor cells. Both injuries led to specific migration of DC to the injured cells within the retina. Conventional markers for MG, CD11b, Iba-1, and F4/80, would not have distinguished this $CD11c^+$ population from resident MG. Consequently, it is uncertain what functions that have been ascribed to MG were instead due to the activity of this population of DC.

Since MG are widely regarded to be the injury-responsive population of myeloid cells in the retina and CNS, we sought strategies that would reveal the presence and response of retinal DC to injury. The optic nerve crush-procedure, which produces a neural injury in which RGC degenerate via apoptosis, is thought to be a potent inducer of MG activation, and is widely used to study the MG response (64, 81-83). An optic nerve crush in the

CD11c-DTR/GFP mice induced a GFP^+CD11b^+ DC response in the NFL, where the DC were found to form intimate contacts with the axons of the injured RGC. The increase of GFP^+CD11b^+ DC at the area of injury was detectable by 2 days, reached a peak at 9 days post-crush, and was still elevated at 60 days post-crush. Interestingly, we found few cells that were GFP^-CD11b^+ in the NFL following optic nerve crush. This observation suggests that this population of DC, rather than MG, is the principal responder to neuronal injury.

Light damage of the retina is another often-used model for activation of a MG response (69, 84-87). The results obtained from the light damage experiments in the CD11c-DTR mice confirm that GFP^+CD11b^+ DC respond to neuronal injury. Continuous exposure of the mice to bright light, at an intensity below that required to produce loss of photoreceptors, led to increased numbers of GFP^+CD11b^+ DC in the OPL, adjacent to the cells that were injured by the light treatment, i.e. the photoreceptor cells.

We found that the GFP^+ DC response to a unilateral optic nerve crush was expressed bilaterally, although the response in the contralateral eye was substantially less robust. Compared to the injured eye, the number of GFP^+CD11b^+ DC was lower in the contralateral NFL, but still significantly higher than normal retina. Most of these cells maintained their ramified morphology. A sympathetic glial response in the contralateral retina to an injury has been previously observed in rodents, most often by documenting a response by cells thought to be MG ($CD11b^+$ cells) after an optic nerve axotomy or crush

(64, 81, 83). Although there is evidence for retino-retinal projections in newborn/young rats (88), that might be injured in an optic nerve crush and give a contralateral stimulus, the number of these projections maintained in adult rats is extremely small (81), and unlikely to account for the response in the contralateral eye. Instead, the uncrossed retinal projections reaching the ipsilateral superior colliculus appear most likely to account for the stimulus in the contralateral retina (81) (Fig. 33). If the retino-retinal projections are, in fact, too few to provide the contralateral injury stimulus, the stimulus for the GFP^+ DC upregulation is likely to result from signals sent via uninjured axons in the superior colliculus to the contralateral retina, and received by the GFP^+ DC. The sympathetic nature of the DC response; i.e., an injury to one retina elicits a DC response in the contralateral retina, suggests that the initial signals that lead to recruitment of DC can be transmitted retrogradely from the projection site, and cautions against the customary use of the opposite eye as a control in studies of retinal injury and physiology.

The GFP^+ DC of retina and brain differed from those in peripheral lymphoid tissue, which showed a direct relationship between the level of CD11c and GFP expression. Further, the GFP^+ DC in lymphoid tissue were $CD45^{hi}$, unlike those from retina and brain, which were $CD45^{med}$. While future studies are needed to dissect out the specific roles of the DC identified in the retina by GFP expression, these studies demonstrate that MG may not be the primary responders of the innate immune response to retinal injury. This is supported by the presence of activated DC around the nerve fibers after optic nerve crush, and their presence in the OPL after light-induced injury. The role of MG in

the injury response will need to be re-evaluated in light of the highly dynamic activity of the GFP^+ DC I have described. In studies not described here, we also found that these cells extensively infiltrated the site of the crush injury in the optic nerve crush procedure, and also densely surrounded the site of a needle stick injury to the brain (data not shown).

Retinal MG have been reported to respond rapidly to retinal laser injury by a mechanism enhanced by CX3CR1. However, the MG population of the quiescent retina was not affected by CX3CR1-deficiency (89, 90). Using the $CX3CR1^+GFP^+$ transgenic mice, the GFP^+ cells were shown to have a highly dynamic morphology, and to migrate rapidly toward the site of injury (90). Whether or not these cells include the CD11c-DTR^+GFP^+ subset of retinal cells we have identified is unknown. Myeloid DC also express GFP in the CX3CR1-GFP mice, and expression of GFP by macrophages/MG and DC in these mice has not been reported to differ in lymphoid tissue, the gut, or the retina (70, 91, 92).

Mice expressing another marker of macrophages and DC, the MacGreen mice [macrophage colony-stimulating factor 1 receptor (CSF-1R)-promoter driven GFP expression], have been used to study myeloid cells in tissues. These mice produce myeloid cells in which virtually all $CD11b^+$, or $F4/80^+$ cells, including myeloid-derived DC, are GFP^+ (93), including the DC of the cornea (94). Since CD11b and F4/80 label MG, as well as the GFP^+ DC we have found in the CD11c-DTR mice, it is unlikely that the retinal DC would be discriminated from MG by GFP expression in the MacGreen mice.

Whether or not the immunologically quiescent retinal microenvironment is sampled by cells with DC-like properties is unclear. The movement of myeloid cells from tissues into the lymphatics is not as well-characterized as migration from blood vessels into tissue. Mature DC in most tissues migrate into lymphatic vessels, and traffic to secondary lymphoid tissue, where they present the antigens gathered in the tissue to T cells. The process is, in part, CCR7 dependent, as DC in CCR7-deficient mice exhibit poor APC trafficking from tissue to lymph nodes. Deficiency in CCR7 ligands, CCL19 and CCL21, produces a similar phenotype (95). In addition, CX3CR1 seems to be involved in MG migration within the retina, as the migration of retinal MG in CX3CR1-/- mice was reduced (96). Together, migration from the blood vessels into tissues, followed by migration from tissues into the lymphatics, account for a substantial portion of the trafficking of myeloid cells throughout the body. However, attempts to demonstrate lymphatic drainage from the retina have not been fruitful. The relevant literature is sparse and unconvincing (97, 98).

If a tissue lacks lymphatics, as appears to be the case for the retina, how does it maintain immune surveillance and homeostasis for its self-antigens? Perivascular cells have been reported by several labs to be phagocytic, and to act as APC (31, 51, 99-101). The results of studies of regulatory T cell generation to antigens of retinal origin (102), suggest local alternative mechanisms for antigen collection and trafficking of those antigens. Since depleting the DTR^+ DC by DTx treatment gave somewhat more severe EAU (personal communication), the role of the resident retinal DC may be immunoregulatory, leading to

inhibition of retinal inflammation and pathogenesis. Conversely, exogenous DC purified from bone marrow and injected into the eye promoted EAU severity (personal communication). The retinal microenvironment may induce a regulatory function on these cells as this result would be consistent with the high levels of TGF-β normally found in the eye (103). However, retinal GFP^+ DC in neither the untreated nor optic nerve injury-treated mice were able to generate significant numbers of T regulatory cells when isolated and tested in vitro. Instead, the GFP^- population from mice that received the optic nerve injury were found to be the most potent generators of T regulatory cells of all the retinal cells analyzed. I have avoided calling the retinal GFP^- population in crushed retinas MG, as it is possible that other cells, recently recruited from the circulation, are the generators of the T regulatory cell population. Nevertheless, it was shown that GFP^+ DC in retinas from mice that had received an optic nerve injury were potent T cell activators.

Most $CD45^+$ cells in adult retina are $CD45^{med}CD11b^+$ MG, and express an additional marker highly associated with CNS microglia, F4/80 (30, 60). Adult retinal cells that phenotypically resemble CNS perivascular cells have been found in much smaller numbers (60, 104-110). Culture of neonatal retinal microglia treated with cytokines revealed expression of molecules associated with antigen presentation (111), and properties associated with DC in neonatal brain (112). However, the relevance of these cells to those in quiet normal adult retina is unknown. In contrast, as shown in this thesis, culturing adult retinal MG with GM/CSF and IFN-γ did not find evidence that retinal MG

were able to present antigen or differentiated into DC-like cells (Fig. 15). The positive results from Matsubara may be explained by the contamination of the tissue with $CD11c^+$ DC in retina (111).

It is widely held that MG in retina (113) and brain (114, 115) turn over very slowly, but possess significant self-renewal potential (79). Conversely, perivascular cells are thought to turn over much more quickly and are derived from circulating precursors, based on studies of bone marrow chimeras (31, 99). We considered the possibility that the GFP^+ cells we have found, based on their potential for rapid turnover, might represent these perivascular cells. Recent results in the literature, and from our lab, indicate that consideration of other factors is needed. While the GFP^+ DC identified in this thesis display a sentinel-like function that can respond rapidly to a challenge, such as optic nerve injury, they exhibit a relatively slow turnover in the absence of a challenge. Further, few of the GFP^+ cells are found in the perivascular morphology, even in quiescent retina, making it unlikely that they represent the perivascular population. Since retinal injury dramatically increased the DC numbers, counts of myeloid cells that do not distinguish retinal DC from MG will be misleading, both in numbers and possibly function.

Another potentially important source of discrepancies in the CNS literature is the highly variable use of radiation/bone marrow chimeras, shielding of tissues, and the effects of reconstitution with a bolus of hematopoietic progenitor cells. Ajami et al. (79) and

Mildner et al. (116) showed that irradiation preconditions the animals. Following transfer of bone marrow, which contains hematopoietic progenitor cells, the migration of bone marrow-derived cells into the CNS increased. In the retina, two recent papers illustrate the effects of radiation dose and differential body shielding. In studies tracking labeled donor progeny of radiation bone marrow chimeras (12 Gy whole body irradiation, unshielded), there was a rapid turnover of MG and perivascular cells that was substantial by 12 - 14 weeks, and nearly complete by 6 months post-bone marrow grafting in normal retina (32). In a similar study also using β-actin-GFP-reporter mice, Kaneko et al. found minimal and temporary influx of donor-derived cells into the quiet retinas of radiation bone marrow chimeras (9 Gy, head-shielded) (117). They further showed that the injury-dependent influx of donor cells eventually resolved, leaving few donor-derived cells in the retina at later time points. Little repopulation of retinal MG by 12 months post-grafting in quiescent retina was found (117). These studies suggest that despite the acquisition of MG-like morphology, the circulating cells recruited by retinal injury appeared to maintain a distinct lineage and temporary residency. The important difference between these studies was the use of shielding to protect the eyes (117), potentially protecting local niches containing myeloid progenitors.

Similar results were found in brain, using a head-shielding strategy (116), and parabiosis, to completely avoid radiation and bone marrow grafting (79). More importantly, the results from parabiosis further implicated ectopic engraftment of progenitor cells contained in the bolus of bone marrow used to reconstitute the irradiated recipients. This

factor appeared even more significant than the irradiation in yielding donor MG in the recipient brain. It now seems possible that these bone marrow cell engraftments may not be unexpected events, but evidence of previously unrecognized local niches for hematopoietic progenitor cells that can be occupied by donor-derived hematopoietic progenitor cells.

Functional differences in the retinal myeloid cell populations are uncertain. For example, MG are reported to possess neuroprotective properties. However, promoting recruitment of hematopoietic progenitor cells into retina by systemic administration of granulocyte colony-stimulating factor (G-CSF) and erythropoietin (EPO) yielded cells in the retina, which assumed a MG morphology and phenotype. These cells were responsive to CXCL12 (SDF-1), and reduced the rate of retinal degeneration in *rd1* mice (42), exhibiting neuroprotective function. However, their identity as resident MG is debatable. Another experiment tested myeloid progenitor cells that were inoculated directly into the vitreous. These cells were found to migrate into the retina, where they expressed markers of MG. These myeloid progenitor cells promoted retinal vascularization in a murine model of hyperoxia-induced ischemic retinopathy (43). Clearly, recruited myeloid-derived cells, "macrophages", exhibit neuroprotective properties in the retina. There is evidence that despite their acquisition of a MG-like phenotype and morphology, these "macrophages" appeared to have distinct lineages that are maintained after resolution of the injury (117). As such, they are not MG.

This thesis has provided multiple lines of evidence that there are at least two separate populations of myeloid-derived cells within retina, cells that use the CD11c promoter of DC to drive GFP reporter expression, and MG. Attempts were made to induce expression of GFP from the transgenic CD11c promoter in cultures of microglia ($CD11b^{+}GFP^{-}$ cells) purified from CD11c-DTR retina, using GM-CSF and/or IFN-γ, but no induction of GFP was found. Parallel positive controls from CD11c-depleted bone marrow from the same animals responded to the same treatment by strongly upregulating GFP (CD11c) expression. *In vivo* experiments confirmed that MG do not give rise to retinal DC. These results are consistent with the hypothesis that these retinal GFP^{+} DC have a lineage distinct from the MG.

Experiments, using chimeric mice, showed that GFP^{+} DC in the host mice declined in retina over time, consistent with a low basal rate of turnover. However, a low number of these GFP^{+} DC was retained. This result came as a surprise as the GFP^{+} DC in the retinas of the bone marrow chimeras should be completely replaced with GFP^{-} DC due to the lack of circulating GFP^{+} DC precursors. Since DC numbers steadily declined, MG did not appear to be a source of the GFP^{+} DC. However, if the precursors were MG, then turnover of the endogenous MG in the chimeras within this time frame could decrease their numbers, reducing the size of the precursor pool. FACS analysis showed that the turnover of endogenous MG was minimal, excluding MG as possible source of retinal GFP^{+} DC. As optic nerve injury stimulated a significant increase in the number of GFP^{+} DC in the ipsilateral retina, and a smaller increase in the contralateral retina, this method

was used to determine if local progenitor cells existed in the retina. Despite the lack of GFP-labeled circulating precursors, a significant elevation of GFP^+ DC was found. This observation was most consistent with the activity of local progenitor cells capable of expanding the number of GFP^+ DC, since DC are not known to be able to expand through the several cycles of division needed to sustain the DC response (76). The literature suggests that hematopoietic progenitor cells circulate in small numbers, and replenish myeloid progenitor cells in peripheral niches (77, 78). Still, the potential remained that a small population of circulating cells had survived the irradiation and was able to reconstitute the GFP^+ DC population in the retina. Experiments did not disprove this hypothesis, but confirmed that local progenitor cells are a source for GFP^+ DC in retina. In addition, preliminary studies of cells expressing markers for hematopoietic progenitor cells (CD34) were found to reside in retinal tissue. Local progenitor cells maintain a long-term ability to produce these DC.

Despite the evidence for local progenitor cells, experiments to determine if the GFP^+ DC could be recruited from circulating precursors clearly supported the contributions of precursors that act via this route, as well. In those studies, a very low turnover of GFP^+ DC was observed in untreated chimeric mice. Again, optic nerve crush injury was used to test if this stimulation could lead to recruitment of GFP^+ DC to the retina, and showed that a high number of GFP^+ DC was found in these retinas. Clearly, the optic nerve injury stimulated recruitment of precursors of GFP^+ DC into the ipsilateral retinas from the circulation and thus, from the transplanted bone marrow. The discussed results show that

retinal GFP^+ DC develop both from circulating precursors and local progenitors, and displayed both a slow turnover in the absence of injury, and a rapid response and turnover following injury. In addition, the experiments showed that the optic nerve crush affected the turnover/loss of MG in the radiation bone marrow chimeras, as host MG was replaced by donor cells at a much faster rate as compared to untreated radiation bone marrow chimeras.

In summary, the studies described in this thesis have revealed a novel myeloid cell population that expresses some properties of DC. While some of these DC have the ramified appearance attributed to MG, others have a perivascular morphology. They appear to be able to adopt both morphologies depending on the status of the retina. These DC are extremely responsive to injury, including an optic nerve crush and photic stress. Even the minimal stimulus of a needle stick to the cornea, that does not touch the retina, generates a sufficient stimulus to cause flux of the retinal GFP^+ DC. Importantly, in CD11c-DTR mice these cells exhibit markers that distinguish them from MG; i.e. GFP (CD11c) and MHC class II, suggesting that some functions usually ascribed to MG are actually due to the population represented by the GFP^+ DC in CD11c-DTR mice.

The retina exhibits a dynamic innate immune response in which this unique GFP^+ population of DC increases and responds early to retinal injury. It was shown that retinal DC are able to present antigen and therefore to activate naïve $CD4^+$ T cells. The GFP^- population in retinas that received a nerve injury was able to suppress T cell activation by

the generation of T regulatory cells. The retinal DC were found to have a dual origin. Some of the retinal GFP^+ DC seem to originate from a local progenitor cell population, while the majority originate from the circulation particularly after retinal injury. Since retina is CNS tissue, there is potential that our findings will apply to the entire CNS, which will advance study of the early events of the innate immune response to CNS injury.

Figure 33. Optic chiasm.

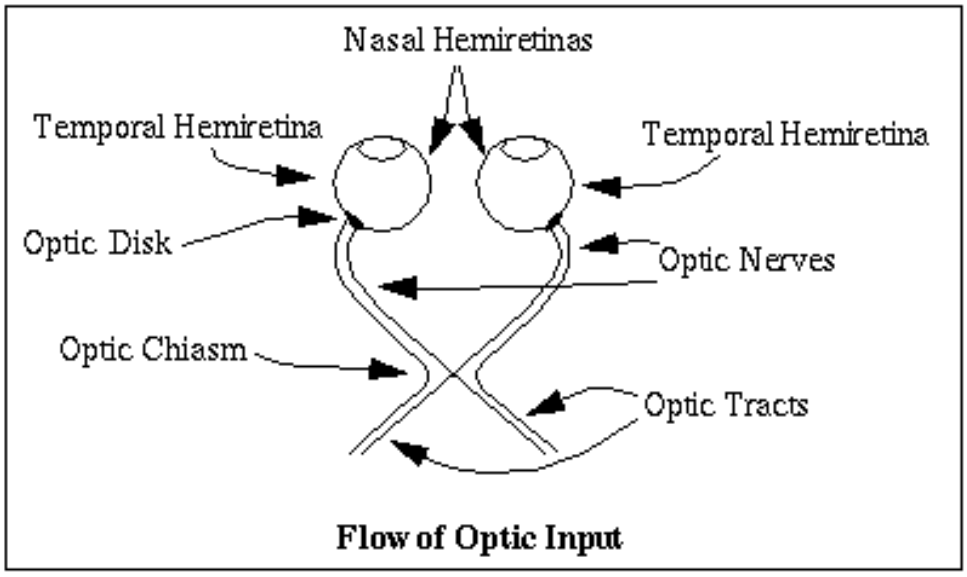

Figure 33. Optic chiasm. The optic chiasm is the part of the brain where the axons of the retinal ganglion cells cross on their paths to the visual centers on the opposite sides of the brain.

REFERENCES

1. Sallusto, F., and A. Lanzavecchia. 1994. Efficient presentation of soluble antigen by cultured human dendritic cells is maintained by granulocyte/macrophage colony-stimulating factor plus interleukin 4 and downregulated by tumor necrosis factor alpha. *Journal of Experimental Medicine* 179:1109-1118.
2. Zinkernagel, R. M., and P. C. Doherty. 1997. The discovery of MHC restriction. *Immunol Today* 18:14-17.
3. Germain, R. N. 1994. MHC-dependent and processing and peptide presentation: providing ligands for T lymphocyte activation. *Cell* 76:287-299.
4. Gromme, M., and J. Neefjes. 2002. Antigen degradation or presentation by MHC class I molecules via classical and non-classical pathways. *Mol Immunol* 39:181-202.
5. Villadangos, J. A. 2001. Presentation of antigens by MHC class II molecules: getting the most out of them. *Mol Immunol* 38:329-346.
6. Liu, Y., and C. A. Janeway, Jr. 1992. Cells that present both specific ligand and costimulatory activity are the most efficient inducers of clonal expansion of normal CD4 T cells. *Proc Natl Acad Sci U S A* 89:3845-3849.
7. Sundstrom, J. B., and A. A. Ansari. 1995. Comparative study of the role of professional versus semiprofessional or nonprofessional antigen presenting cells in the rejection of vascularized organ allografts. *Transpl Immunol* 3:273-289.
8. Lee, H. K., and A. Iwasaki. 2007. Innate control of adaptive immunity: dendritic cells and beyond. *Semin Immunol* 19:48-55.
9. Villadangos, J. A., and P. Schnorrer. 2007. Intrinsic and cooperative antigen-presenting functions of dendritic-cell subsets in vivo. *Nat Rev Immunol* 7:543-555.
10. Liu, K., and M. C. Nussenzweig. 2010. Origin and development of dendritic cells. *Immunol Rev* 234:45-54.
11. Steinman, R. M., and Z. A. Cohn. 1973. Identification of a novel cell type in peripheral lymphoid organs of mice. I. Morphology, quantitation, tissue distribution. *J Exp Med* 137:1142-1162.
12. Steinman, R. M., and M. D. Witmer. 1978. Lymphoid dendritic cells are potent stimulators of the primary mixed leukocyte reaction in mice. *Proc Natl Acad Sci U S A* 75:5132-5136.
13. Steinman, R. M., and Z. A. Cohn. 1974. Identification of a novel cell type in peripheral lymphoid organs of mice. II. Functional properties in vitro. *J Exp Med* 139:380-397.
14. Pulendran, B., J. L. Smith, G. Caspary, K. Brasel, D. Pettit, E. Maraskovsky, and C. R. Maliszewski. 1999. Distinct dendritic cell subsets differentially regulate the class of immune response in vivo. *Proc Natl Acad Sci U S A* 96:1036-1041.
15. Daro, E., B. Pulendran, K. Brasel, M. Teepe, D. Pettit, D. H. Lynch, D. Vremec, L. Robb, K. Shortman, H. J. McKenna, C. R. Maliszewski, and E. Maraskovsky. 2000. Polyethylene glycol-modified GM-CSF expands CD11b(high)CD11c(high)

but notCD11b(low)CD11c(high) murine dendritic cells in vivo: a comparative analysis with Flt3 ligand. *J Immunol* 165:49-58.
16. Maraskovsky, E., K. Brasel, M. Teepe, E. R. Roux, S. D. Lyman, K. Shortman, and H. J. McKenna. 1996. Dramatic increase in the numbers of functionally mature dendritic cells in Flt3 ligand-treated mice: multiple dendritic cell subpopulations identified. *J Exp Med* 184:1953-1962.
17. Pulendran, B., J. Lingappa, M. K. Kennedy, J. Smith, M. Teepe, A. Rudensky, C. R. Maliszewski, and E. Maraskovsky. 1997. Developmental pathways of dendritic cells in vivo: distinct function, phenotype, and localization of dendritic cell subsets in FLT3 ligand-treated mice. *J Immunol* 159:2222-2231.
18. Traver, D., K. Akashi, M. Manz, M. Merad, T. Miyamoto, E. G. Engleman, and I. L. Weissman. 2000. Development of CD8alpha-positive dendritic cells from a common myeloid progenitor. *Science* 290:2152-2154.
19. del Hoyo, G. M., P. Martin, H. H. Vargas, S. Ruiz, C. F. Arias, and C. Ardavin. 2002. Characterization of a common precursor population for dendritic cells. *Nature* 415:1043-1047.
20. Zuniga, E. I., D. B. McGavern, J. L. Pruneda-Paz, C. Teng, and M. B. Oldstone. 2004. Bone marrow plasmacytoid dendritic cells can differentiate into myeloid dendritic cells upon virus infection. *Nat Immunol* 5:1227-1234.
21. Rissoan, M.-C., V. Soumelis, N. Kadowski, G. Grouard, F. Briere, R. d. W. Malefyt, and Y.-J. Liu. 1999. Reciprocal Control of T Helper Cell and Dendritic Cell Differentiation. *Science* 283:1183-1186.
22. Gilliet, M., and Y. J. Liu. 2002. Generation of human CD8 T regulatory cells by CD40 ligand-activated plasmacytoid dendritic cells. *J Exp Med* 195:695-704.
23. Auffray, C., M. H. Sieweke, and F. Geissmann. 2009. Blood monocytes: development, heterogeneity, and relationship with dendritic cells. *Annu Rev Immunol* 27:669-692.
24. Randolph, G. J., K. Inaba, D. F. Robbiani, R. M. Steinman, and W. A. Muller. 1999. Differentiation of phagocytic monocytes into lymph node dendritic cells in vivo. *Immunity* 11:753-761.
25. Pulendran, B., P. Kumar, C. W. Cutler, M. Mohamadzadeh, T. Van Dyke, and J. Banchereau. 2001. Lipopolysaccharides from distinct pathogens induce different classes of immune responses in vivo. *J Immunol* 167:5067-5076.
26. Jotwani, R., B. Pulendran, S. Agrawal, and C. W. Cutler. 2003. Human dendritic cells respond to Porphyromonas gingivalis LPS by promoting a Th2 effector response in vitro. *Eur J Immunol* 33:2980-2986.
27. Jonuleit, H., E. Schmitt, G. Schuler, J. Knop, and A. H. Enk. 2000. Induction of interleukin 10-producing, nonproliferating CD4(+) T cells with regulatory properties by repetitive stimulation with allogeneic immature human dendritic cells. *J Exp Med* 192:1213-1222.
28. Steel, C. D., S. M. Hahto, and R. P. Ciavarra. 2009. Peripheral dendritic cells are essential for both the innate and adaptive antiviral immune responses in the central nervous system. *Virology* 387:117-126.

29. Dick, A. D. 1999. Immune regulation of uveoretinal inflammation. *Dev. Ophthalmol.* 30:187-202.
30. Gregerson, D. S., T. N. Sam, and S. W. McPherson. 2004. The antigen-presenting activity of fresh, adult parenchymal microglia and perivascular cells from retina. *J. Immunol.* 172:6587-6597.
31. Hickey, W., and H. Kimura. 1988. Perivascular microglial cells of the CNS are bone marrow-derived and present antigen in vivo. *Science* 239:290-292.
32. Xu, H., M. Chen, E. J. Mayer, J. V. Forrester, and A. D. Dick. 2007. Turnover of resident retinal microglia in the normal adult mouse. *Glia* 55:1189-1198.
33. Lehmann, U., N. D. Heuss, S. W. McPherson, H. Roehrich, and D. S. Gregerson. 2010. Dendritic cells are early responders to retinal injury. *Neurobiol Dis*.
34. Graeber, M. B., and W. J. Streit. 2010. Microglia: biology and pathology. *Acta Neuropathol* 119:89-105.
35. Kim, S. U., and J. de Vellis. 2005. Microglia in health and disease. *J Neurosci Res* 81:302-313.
36. Garden, G. A., and T. Moller. 2006. Microglia biology in health and disease. *J Neuroimmune Pharmacol* 1:127-137.
37. Streit, W. J., R. E. Mrak, and W. S. Griffin. 2004. Microglia and neuroinflammation: a pathological perspective. *J Neuroinflammation* 1:14.
38. Sanders, V. M., and K. J. Jones. 2006. Role of immunity in recovery from a peripheral nerve injury. *J Neuroimmune Pharmacol* 1:11-19.
39. Lehnardt, S., E. Schott, T. Trimbuch, D. Laubisch, C. Krueger, G. Wulczyn, R. Nitsch, and J. R. Weber. 2008. A vicious cycle involving release of heat shock protein 60 from injured cells and activation of toll-like receptor 4 mediates neurodegeneration in the CNS. *J Neurosci* 28:2320-2331.
40. Wakselman, S., C. Bechade, A. Roumier, D. Bernard, A. Triller, and A. Bessis. 2008. Developmental neuronal death in hippocampus requires the microglial CD11b integrin and DAP12 immunoreceptor. *J Neurosci* 28:8138-8143.
41. Streit, W. J. 2005. Microglia and neuroprotection: implications for Alzheimer's disease. *Brain Res Brain Res Rev* 48:234-239.
42. Sasahara, M., A. Otani, A. Oishi, H. Kojima, Y. Yodoi, T. Kameda, H. Nakamura, and N. Yoshimura. 2008. Activation of bone marrow-derived microglia promotes photoreceptor survival in inherited retinal degeneration. *The American journal of pathology* 172:1693-1703.
43. Ritter, M. R., E. Banin, S. K. Moreno, E. Aguilar, M. I. Dorrell, and M. Friedlander. 2006. Myeloid progenitors differentiate into microglia and promote vascular repair in a model of ischemic retinopathy. *J Clin Invest* 116:3266-3276.
44. Kivisakk, P., J. Imitola, S. Rasmussen, W. Elyaman, B. Zhu, R. M. Ransohoff, and S. J. Khoury. 2009. Localizing central nervous system immune surveillance: meningeal antigen-presenting cells activate T cells during experimental autoimmune encephalomyelitis. *Ann Neurol* 65:457-469.
45. Gregerson, D. S., W. F. Obritsch, S. P. Fling, and J. D. Cameron. 1986. S-antigen-specific rat T cell lines recognize peptide fragments of S-antigen and mediate experimental autoimmune uveoretinitis and pinealitis. *J Immunol* 136:2875-2882.

46. McPherson, S. W., N. D. Heuss, H. Roehrich, and D. S. Gregerson. 2006. Bystander killing of neurons by cytotoxic T cells specific for a glial antigen. *Glia* 53:457-466.
47. McPherson, S. W., J. Yang, C. C. Chan, C. Dou, and D. S. Gregerson. 2003. Resting CD8 T cells recognize beta-galactosidase expressed in the immune-privileged retina and mediate autoimmune disease when activated. *Immunology* 110:386-396.
48. Caspi, R. R., F. G. Roberge, C. C. Chan, B. Wiggert, G. J. Chader, L. A. Rozenszajn, Z. Lando, and R. B. Nussenblatt. 1988. A new model of autoimmune disease. Experimental autoimmune uveoretinitis induced in mice with two different retinal antigens. *Journal of Immunology* 140:1490-1495.
49. Ben-Nun, A., H. Wekerle, and I. Cohen. 1981. The rapid isolation of clonable antigen-specific T lymphocyte lines capable of mediating autoimmune encephalomyelitis. *European Journal of Immunology* 11:195-199.
50. Xu, H., R. Dawson, J. V. Forrester, and J. Liversidge. 2007. Identification of novel dendritic cell populations in normal mouse retina. *Invest. Ophthalmol. Vis. Sci.* 48:1701-1710.
51. Greter, M., F. L. Heppner, M. P. Lemos, B. M. Odermatt, N. Goebels, T. Laufer, R. J. Noelle, and B. Becher. 2005. Dendritic cells permit immune invasion of the CNS in an animal model of multiple sclerosis. *Nat Med* 11:328-334. Epub 2005 Feb 2027.
52. McMahon, E. J., S. L. Bailey, and S. D. Miller. 2006. CNS dendritic cells: critical participants in CNS inflammation? *Neurochem Int* 49:195-203.
53. Gregerson, D. S., and H. Kawashima. 2004. APC derived from donor splenocytes support retinal autoimmune disease in allogeneic recipients. *J. Leukoc. Biol.* 76:383-387.
54. Niederkorn, J. Y. 2006. See no evil, hear no evil, do no evil: the lessons of immune privilege. *Nat Immunol* 7:354-359.
55. Simpson, E. 2006. A historical perspective on immunological privilege. *Immunol Rev* 213:12-22.
56. Hong, S., and L. Van Kaer. 1999. Immune privilege: keeping an eye on natural killer T cells. *J Exp Med* 190:1197-1200.
57. Green, D. R., and C. F. Ware. 1997. Fas-ligand: privilege and peril. *Proc Natl Acad Sci U S A* 94:5986-5990.
58. Jiang, H. R., L. Lumsden, and J. V. Forrester. 1999. Macrophages and dendritic cells in IRBP-induced experimental autoimmune uveoretinitis in B10RIII mice. *Invest. Ophthalmol. Vis. Sci.* 40:3177-3185.
59. Brasel, K., T. De Smedt, J. L. Smith, and C. R. Maliszewski. 2000. Generation of murine dendritic cells from flt3-ligand-supplemented bone marrow cultures. *Blood* 96:3029-3039.
60. Gregerson, D. S., and J. Yang. 2003. CD45-positive cells of the retina and their responsiveness to in vivo and in vitro treatment with IFN-gamma or anti-CD40. *Invest. Ophthalmol. Vis. Sci.* 44:3083-3093.

61. Jung, S., D. Unutmaz, P. Wong, G. Sano, K. De los Santos, T. Sparwasser, S. Wu, S. Vuthoori, K. Ko, F. Zavala, E. G. Pamer, D. R. Littman, and R. A. Lang. 2002. In vivo depletion of CD11c(+) dendritic cells abrogates priming of CD8(+) T cells by exogenous cell-associated antigens. *Immunity* 17:211-220.
62. Yoles, E., and M. Schwartz. 1998. Elevation of intraocular glutamate levels in rats with partial lesion of the optic nerve. *Arch Ophthalmol* 116:906-910.
63. Sautter, J., and B. A. Sabel. 1993. Recovery of brightness discrimination in adult rats despite progressive loss of retrogradely labelled retinal ganglion cells after controlled optic nerve crush. *Eur J Neurosci* 5:680-690.
64. Panagis, L., S. Thanos, D. Fischer, and C. R. Dermon. 2005. Unilateral optic nerve crush induces bilateral retinal glial cell proliferation. *Eur. J. Neurosci.* 21:2305-2309.
65. Bodeutsch, N., H. Siebert, C. Dermon, and S. Thanos. 1999. Unilateral injury to the adult rat optic nerve causes multiple cellular responses in the contralateral site. *J Neurobiol* 38:116-128.
66. Li, Y., C. L. Schlamp, and R. W. Nickells. 1999. Experimental induction of retinal ganglion cell death in adult mice. *Invest. Ophthalmol. Vis. Sci.* 40:1004-1008.
67. LaVail, M. M., G. M. Gorrin, M. A. Repaci, L. A. Thomas, and H. M. Ginsberg. 1987. Genetic regulation of light damage to photoreceptors. *Investigative ophthalmology & visual science* 28:1043-1048.
68. Winkler, B. 1981. Glycolytic and oxidative metabolism in relation to retinal function. *J. Gen. Physiol.* 77:667-692.
69. Santos, A. M., D. Martin-Oliva, R. M. Ferrer-Martin, M. Tassi, R. Calvente, A. Sierra, M. C. Carrasco, J. L. Marin-Teva, J. Navascues, and M. A. Cuadros. 2010. Microglial response to light-induced photoreceptor degeneration in the mouse retina. *The Journal of comparative neurology* 518:477-492.
70. Kezic, J., H. Xu, H. R. Chinnery, C. C. Murphy, and P. G. McMenamin. 2008. Retinal microglia and uveal tract dendritic cells and macrophages are not CX3CR1 dependent in their recruitment and distribution in the young mouse eye. *Investigative ophthalmology & visual science* 49:1599-1608.
71. Garcia-Valenzuela, E., S. C. Sharma, and A. L. Pina. 2005. Multilayered retinal microglial response to optic nerve transection in rats. *Mol Vis* 11:225-231.
72. Oishi, A., A. Otani, M. Sasahara, H. Kojima, H. Nakamura, Y. Yodoi, and N. Yoshimura. 2008. Granulocyte colony-stimulating factor protects retinal photoreceptor cells against light-induced damage. *Investigative ophthalmology & visual science* 49:5629-5635.
73. O'Driscoll, C., J. O'Connor, C. J. O'Brien, and T. G. Cotter. 2008. Basic fibroblast growth factor-induced protection from light damage in the mouse retina in vivo. *J Neurochem* 105:524-536.
74. Mittag, T. W., A. U. Bayer, and M. M. LaVail. 1999. Light-induced retinal damage in mice carrying a mutated SOD I gene. *Experimental eye research* 69:677-683.

75. Hermiston, M. L., Z. Xu, and A. Weiss. 2003. CD45: a critical regulator of signaling thresholds in immune cells. *Annu Rev Immunol* 21:107-137.
76. Kamath, A. T., S. Henri, F. Battye, D. F. Tough, and K. Shortman. 2002. Developmental kinetics and lifespan of dendritic cells in mouse lymphoid organs. *Blood* 100:1734-1741.
77. Massberg, S., P. Schaerli, I. Knezevic-Maramica, M. Kollnberger, N. Tubo, E. A. Moseman, I. V. Huff, T. Junt, A. J. Wagers, I. B. Mazo, and U. H. von Andrian. 2007. Immunosurveillance by hematopoietic progenitor cells trafficking through blood, lymph, and peripheral tissues. *Cell* 131:994-1008.
78. Wright, D. E., A. J. Wagers, A. P. Gulati, F. L. Johnson, and I. L. Weissman. 2001. Physiological migration of hematopoietic stem and progenitor cells. *Science* 294:1933-1936.
79. Ajami, B., J. L. Bennett, C. Krieger, W. Tetzlaff, and F. M. Rossi. 2007. Local self-renewal can sustain CNS microglia maintenance and function throughout adult life. *Nat Neurosci* 10:1538-1543.
80. Bhattacharya, D., A. Czechowicz, A. G. Ooi, D. J. Rossi, D. Bryder, and I. L. Weissman. 2009. Niche recycling through division-independent egress of hematopoietic stem cells. *The Journal of experimental medicine* 206:2837-2850.
81. Macharadze, T., J. Goldschmidt, M. Marunde, T. Wanger, H. Scheich, W. Zuschratter, E. D. Gundelfinger, and M. R. Kreutz. 2009. Interretinal transduction of injury signals after unilateral optic nerve crush. *Neuroreport* 20:301-305.
82. Bodeutsch, N., and S. Thanos. 2000. Migration of phagocytotic cells and development of the murine intraretinal microglial network: an in vivo study using fluorescent dyes. *Glia* 32:91-101.
83. Bodeutsch, N., H. Siebert, C. Dermon, and S. Thanos. 1999. Unilateral injury to the adult rat optic nerve causes multiple cellular responses in the contralateral site. *J. Neurobiol.* 38:116-128.
84. Zhang, C., J. K. Shen, T. T. Lam, H. Y. Zeng, S. K. Chiang, F. Yang, and M. O. Tso. 2005. Activation of microglia and chemokines in light-induced retinal degeneration. *Mol Vis* 11:887-895.
85. Zhang, C., B. Lei, T. T. Lam, F. Yang, D. Sinha, and M. O. Tso. 2004. Neuroprotection of photoreceptors by minocycline in light-induced retinal degeneration. *Invest Ophthalmol Vis Sci* 45:2753-2759.
86. Ni, Y. Q., G. Z. Xu, W. Z. Hu, L. Shi, Y. W. Qin, and C. D. Da. 2008. Neuroprotective effects of naloxone against light-induced photoreceptor degeneration through inhibiting retinal microglial activation. *Investigative ophthalmology & visual science* 49:2589-2598.
87. Harada, T., C. Harada, S. Kohsaka, E. Wada, K. Yoshida, S. Ohno, H. Mamada, K. Tanaka, L. F. Parada, and K. Wada. 2002. Microglia-Muller glia cell interactions control neurotrophic factor production during light-induced retinal degeneration. *J Neurosci* 22:9228-9236.
88. Muller, M., and H. Hollander. 1988. A small population of retinal ganglion cells projecting to the retina of the other eye. An experimental study in the rat and the rabbit. *Exp Brain Res* 71:611-617.

89. Liang, K. J., J. E. Lee, Y. D. Wang, W. Ma, A. M. Fontainhas, R. N. Fariss, and W. T. Wong. 2009. Regulation of dynamic behavior of retinal microglia by CX3CR1 signaling. *Investigative ophthalmology & visual science* 50:4444-4451.
90. Lee, J. E., K. J. Liang, R. N. Fariss, and W. T. Wong. 2008. Ex vivo dynamic imaging of retinal microglia using time-lapse confocal microscopy. *Investigative ophthalmology & visual science* 49:4169-4176.
91. del Rio, M. L., J. I. Rodriguez-Barbosa, J. Bolter, M. Ballmaier, O. Dittrich-Breiholz, M. Kracht, S. Jung, and R. Forster. 2008. CX3CR1+ c-kit+ bone marrow cells give rise to CD103+ and CD103- dendritic cells with distinct functional properties. *J Immunol* 181:6178-6188.
92. Niess, J. H., and G. Adler. 2010. Enteric flora expands gut lamina propria CX3CR1+ dendritic cells supporting inflammatory immune responses under normal and inflammatory conditions. *J Immunol* 184:2026-2037.
93. MacDonald, K. P., V. Rowe, H. M. Bofinger, R. Thomas, T. Sasmono, D. A. Hume, and G. R. Hill. 2005. The colony-stimulating factor 1 receptor is expressed on dendritic cells during differentiation and regulates their expansion. *J Immunol* 175:1399-1405.
94. Chinnery, H. R., E. Pearlman, and P. G. McMenamin. 2008. Cutting edge: Membrane nanotubes in vivo: a feature of MHC class II+ cells in the mouse cornea. *J Immunol* 180:5779-5783.
95. Forster, R., A. C. Davalos-Misslitz, and A. Rot. 2008. CCR7 and its ligands: balancing immunity and tolerance. *Nat Rev Immunol* 8:362-371.
96. Raoul, W., N. Keller, M. Rodero, F. Behar-Cohen, F. Sennlaub, and C. Combadiere. 2008. Role of the chemokine receptor CX3CR1 in the mobilization of phagocytic retinal microglial cells. *J Neuroimmunol* 198:56-61.
97. Egan, R. M., C. Yorkey, R. Black, W. K. Loh, J. L. Stevens, E. Storozynsky, E. M. Lord, J. G. Frelinger, and J. G. Woodward. 2000. In vivo behavior of peptide-specific T cells during mucosal tolerance induction: antigen introduced through the mucosa of the conjunctiva elicits prolonged antigen-specific T cell priming followed by anergy. *Journal of Immunology* 164:4543-4550.
98. Egan, R. M., C. Yorkey, R. Black, W. K. Loh, J. L. Stevens, and J. G. Woodward. 1996. Peptide-specific T cell clonal expansion in vivo following immunization in the eye, an immune-privileged site. *Journal of Immunology* 157:2262-2271.
99. Bechmann, I., E. Kwidzinski, A. D. Kovac, E. Simburger, T. Horvath, U. Gimsa, U. Dirnagl, J. Priller, and R. Nitsch. 2001. Turnover of rat brain perivascular cells. *Exp Neurol* 168:242-249.
100. Bechmann, I., J. Priller, A. Kovac, M. Bontert, T. Wehner, F. F. Klett, J. Bohsung, M. Stuschke, U. Dirnagl, and R. Nitsch. 2001. Immune surveillance of mouse brain perivascular spaces by blood-borne macrophages. *Eur J Neurosci* 14:1651-1658.
101. Priller, J., A. Flugel, T. Wehner, M. Boentert, C. A. Haas, M. Prinz, F. Fernandez-Klett, K. Prass, I. Bechmann, B. A. de Boer, M. Frotscher, G. W. Kreutzberg, D. A. Persons, and U. Dirnagl. 2001. Targeting gene-modified hematopoietic cells to

the central nervous system: use of green fluorescent protein uncovers microglial engraftment. *Nat Med* 7:1356-1361.
102. McPherson, S. W., N. D. Heuss, and D. S. Gregerson. 2009. Lymphopenia-induced proliferation is a potent activator for CD4+ T cell mediated autoimmune disease in the retina. *J. Immunol.* 182:969-979.
103. Saika, S. 2006. TGFbeta pathobiology in the eye. *Lab Invest* 86:106-115.
104. Cuff, C. A., J. W. Berman, and C. F. Brosnan. 1996. The ordered array of perivascular macrophages is disrupted by IL-1- induced inflammation in the rabbit retina. *Glia* 17:307-316.
105. Dick, A. D., A. L. Ford, J. V. Forrester, and J. D. Sedgwick. 1995. Flow cytometric identification of a minority population of MHC class II positive cells in the normal rat retina distinct from CD45lowCD11b/c+CD4low parenchymal microglia. *Br. J. Ophthalmol.* 79:834-840.
106. Hu, P., J. D. Pollard, and T. Chan-Ling. 2000. Breakdown of the blood-retinal barrier induced by activated T cells of nonneural specificity. *Am J Pathol* 156:1139-1149.
107. Zhang, J., G. S. Wu, S. Ishimoto, G. Pararajasegaram, and N. A. Rao. 1997. Expression of major histocompatibility complex molecules In rodent retina - immunohistochemical study. *Invest. Ophthalmol. Vis. Sci.* 38:1848-1857.
108. Penfold, P. L., S. C. Liew, M. C. Madigan, and J. M. Provis. 1997. Modulation of major histocompatibility complex class II expression in retinas with age-related macular degeneration. *Invest Ophthalmol Vis Sci* 38:2125-2133.
109. Zhang, C., and M. O. Tso. 2003. Characterization of activated retinal microglia following optic axotomy. *J. Neurosci. Res.* 73:840-845.
110. Chen, L., P. Yang, and A. Kijlstra. 2002. Distribution, markers, and functions of retinal microglia. *Ocul Immunol Inflamm* 10:27-39.
111. Matsubara, T., G. Pararajasegaram, G. S. Wu, and N. A. Rao. 1999. Retinal microglia differentially express phenotypic markers of antigen-presenting cells in vitro. *Investigative Ophthalmology & Visual Science* 40:3186-3193.
112. Santambrogio, L., S. L. Belyanskaya, F. R. Fischer, B. Cipriani, C. F. Brosnan, P. Ricciardi-Castagnoli, L. J. Stern, J. L. Strominger, and R. Riese. 2001. Developmental plasticity of CNS microglia. *Proc Natl Acad Sci U S A* 98:6295-6300.
113. Kezic, J., and P. G. McMenamin. 2008. Differential turnover rates of monocyte-derived cells in varied ocular tissue microenvironments. *J Leukoc Biol* 84:721-729.
114. Gehrmann, J., Y. Matsumoto, and G. W. Kreutzberg. 1995. Microglia: intrinsic immuneffector cell of the brain. *Brain Research - Brain Research Reviews* 20:269-287.
115. Lassmann, H., M. Schmied, K. Vass, and W. F. Hickey. 1993. Bone marrow derived elements and resident microglia in brain inflammation. *Glia* 7:19-24.
116. Mildner, A., H. Schmidt, M. Nitsche, D. Merkler, U. K. Hanisch, M. Mack, M. Heikenwalder, W. Bruck, J. Priller, and M. Prinz. 2007. Microglia in the adult

brain arise from Ly-6ChiCCR2+ monocytes only under defined host conditions. *Nature neuroscience* 10:1544-1553.

117. Kaneko, H., K. M. Nishiguchi, M. Nakamura, S. Kachi, and H. Terasaki. 2008. Characteristics of Bone Marrow-Derived Microglia in the Normal and Injured Retina. *Investigative ophthalmology & visual science* 49:4162-4168.